

# AdaPtive Noisy Data Augmentation (PANDA) for Simultaneous Construction Multiple Graph Models

Yinan Li<sup>1</sup>, Xiao Liu<sup>2</sup>, and Fang Liu<sup>1\*</sup>

<sup>1</sup> Department of Applied and Computational Mathematics and Statistics

<sup>2</sup> Department of Psychology

University of Notre Dame, Notre Dame, IN 46556, U.S.A.

## Abstract

We extend the data augmentation technique (PANDA) by Li et al. (2018) for regularizing single graph model estimations to jointly learning the structures of multiple graphs. Our proposed approach provides an unified framework to effectively jointly train multiple graphical models, regardless of the types of nodes. We design and introduce two types of noises to augment the observed data. The first type of noises is to regularize the estimation of each graph while the second type of noises promotes either the structural similarities, referred as the *joint group lasso (JGL)* regularization, or numerical similarities, referred as the *joint fused ridge (JFR)* regularization, among the edges in the same position across multiple graphs. The computation in PANDA is straightforward and only involves obtaining maximum likelihood estimator in generalized linear models (GLMs) in an iterative manner. We also extend the JGL and JFR regularization beyond the graphical model settings to variable selection and estimation in GLMs. The multiple graph version of PANDA enjoys the theoretical properties established for single graphs including the almost sure (a.s) convergence of the noise-augmented loss function to its expectation and the a.s convergence of the minimizer of the former to the minimizer of the latter. The simulation studies suggest PANDA is non-inferior to existing joint estimation approaches in constructing multiple Gaussian graphical models (GGMs), and significantly improves over the differencing approach over separately estimated graphs in multiple Poisson graphical models (PGMs). We also applied PANDA to a real-life lung cancer microarray data to simultaneously construct four protein networks.

**keywords:** generalized linear models (GLMs), adjacency matrix, sparsity, similarity, sparse group lasso (SGL), sparse fused ridge (SFR)

---

\*Corresponding author email: fang.liu.131@nd.edu

# 1 Introduction

Undirected graphical models (UGMs) are used to capture the bilateral conditional dependency structure among a set of variables or nodes. This structure can be mathematically expressed by the  $p \times p$  symmetric adjacency matrix  $\mathbf{A}$ . If the entry  $A_{ij}$  is 0, then nodes  $i$  and  $j$  are conditionally independent; otherwise, there is a conditional dependency and an edge is drawn between the two nodes graphically. In recent years, there are a lot of research interests in constructing multiple graphs based on data collected from a set of nodes but in different conditions. For example, medical researchers may measure gene expression from tumor samples and normal samples, and they are interested how cancer affects the connection pattern among the genes (nodes).

Real-life graphs are often believed to take on sparse structures, especially for large-scale networks; and in the case of multiple graphs, the change of conditions is expected to only affect a small subset of edges while leaving the majority of connection patterns intact across the graphs. To accommodate these real-life expectation, sparsity-promoting regularization is often applied when constructing both single and multiple graphs.

In the single graph setting, neighborhood selection (NS) is a popular and simple method to recover the structures of UGMs that guarantees the structure consistency (Yang et al., 2012, 2015a). When the underlying conditional distribution of one node given all others can be modeled by the exponential family, NS transforms the original graph construction problem into building  $p$  generalized linear regression models (GLMs), where sparsity regularization, such as  $l_1$  can be applied directly. Methodology and theory have been developed in linear regression for Gaussian graphical models (GGMs) (Yuan, 2010); logistic regression for Ising models (Ravikumar et al., 2010), Bernoulli nodes (Hoffing and Tibshirani, 2009), and categorical nodes (Jalali et al., 2011; Kuang et al., 2017); and Poisson regression for count nodes (Allen and Liu, 2012); as well as mixed graph models (MGMs) when there are different node types in one UGM (Yang et al., 2012; Fellinghauer et al., 2013; Yang et al., 2014). Li et al. (2018) also provide the a data Augmentation approach, named PANDA, for constructing single UGMs in general that offers a wide spectrum of regularization effects with properly designed augmented noise terms.

For multiple graph construction, the naive approach would be to estimate each graph separately, and then compare the structures in a post-hoc manner for differences. A better approach is to jointly estimating multiple graphs simultaneously, acknowledging and leveraging the expectation that the structures would largely remain consistent across the multiple graphs while the discrepancy is in the minority. Hoefling (2009) applied the fused lasso (FL) penalty to the regression coefficients in the framework of NS to encourage similar networks structure across graphs. Danaher et al. (2014) proposed the fused graphical lasso and group graphical lasso with the pairwise fused penalty and the group penalty, respectively, to directly estimate the precision matrices simultaneously. Yang et al. (2015b) considered the sequential version of fused graphical lasso penalty favorable for training time-evolving graphs.

All the above listed work in the multiple graph setting focuses on GGMs where the nodes are assumed to follow multivariate Gaussian distributions. There is much less work when it comes to jointly training multiple UGMs with non-Gaussian nodes. The only related work we could locate is by Zhang et al. (2017), where the group lasso and fused lasso penalties developed by Danaher et al. (2014) for GGMs are extended to graph models with a mixture of Bernoulli and Gaussian nodes using a pseudo-likelihood approach.

In this paper, we aim to develop an approach that provides an unified framework to effectively jointly train multiple UGMs, regardless of the types of nodes, that satisfy the expectation that both the connections in single graph and different connections across multiple graphs are sparse. Toward

that end, we will extend the PANDA technique developed by Li et al. (2018) for regularizing single UGM estimation to jointly learning structures of multiple graphs. Specifically, we will design and introduce two types of noises to be tagged onto the original observed data when employing PANDA for multiple graph estimation. The first type of noises, similar to those presented in Li et al. (2018), is to regularize the estimation of each graph. We then propose a second type of noises to promote either structural similarities, referred as the *joint group lasso (JGL)*, or numerical similarities, referred as the *joint fused ridge (JFR)*, among the edges across multiple graphs. The augmented data in each graph are combined across all graphs and GLMs are fitted node by node on the augmented combined data to simultaneously constructing the graphs. Our contributions are summarized as follows.

- To the best our knowledge, our extension of PANDA to the multiple graph setting offers the first general framework to jointly construct multiple UGMs in general (GGMs and MGMs included), as long as each node in the graphs given the other nodes can be modelled by the Exponential family and the GLMs.
- Both the JGL and JFR regularization terms are convex and PANDA recasts the optimization problem as solving maximum likelihood estimation (MLE) from GLMs on noise-augmented data without employing any complicated optimization algorithms, as long as  $\sum_{l=1}^q n^{(l)} + n_{e,1} + n_{e,2} > 3p$  ( $n^{(l)}$  is the sample size of graph  $l$ ,  $q$  of the number of graphs,  $n_{e,1}$  and  $n_{e,2}$  are the sizes of the two types of augmented noises, and  $p$  is the number of nodes in each graph). As such, the computation in PANDA is straightforward and only involves obtaining MLE in GLMs in an iterative manner. The variances of the augmented noises are adaptive to the most up-to-date parameter estimates throughout iterations until convergence.
- When all the graphs are GGMs, besides PANDA-NS, we also develop PANDA-CD that is based on the Cholesky decomposition (CD) of the precision matrices as Huang et al. (2006) proposed for single GGM estimation, and PANDA-SCIO that recasts the problem as a regularized quadratic optimization without employing the Gaussian likelihood, inspired by the Sparse Column-wise Inverse Operator (SCIO) for single GGM estimation (Liu and Xi, 2015).
- We offer a Bayesian interpretation for PANDA in joint estimating multiple UGMs and connect PANDA with the empirical Bayes and *maximum a posteriori probability (MAP)* estimate in each iteration of PANDA.
- We extend the JGL and JFR regularization beyond the graphical model construction to variable selection and estimation in GLMs. In such case, the JGL is equivalent to the sparse group lasso (SGL) regularization (Simon et al., 2013). We propose and coin the term “sparse fused ridge (SFR)” as the equivalence to JFR in the regression framework, including the Bayesian version of SFR.
- The theoretical properties established by Li et al. (2018) in the single graph setting also apply to the multiple graph case, including the almost sure (a.s) convergence of the noise-augmented loss function to its expectation and the a.s convergence of the minimizer of the former to the minimizer of the latter. This is because PANDA, operationally, still treats the combined augmented data across multiple graphs as from a single graph, while imposing the right regularization effect on the right set of the graph parameters with the cleverly designed noises.

The rest of the paper is organized as follows. Section 2 presents multiple PANDA techniques in joint estimation of multiple UGMs and GGMs with two types of regularization for promoting the structural similarity across multiple UGMs, and also provides PANDA a Bayesian interpretation in the multiple graph setting. Section 3 applies PANDA in simulated multiple graphs and compares its performance against the commonly used estimation approaches. Section 4 applies PANDA to a real-life lung cancer microarray data to construct four GGMs simultaneously. The paper concludes in Section 5 with some final remarks.

## 2 PANDA for Simultaneous Construction of Multiple Graphs

In this section, we present the PANDA technique for constructing and differentiating multiple UGMs. The key component in the extension of the PANDA approach to the multiple graph setting is to design a second type of noises that promoting structural or numerical similarities among the edges in the same position across graphs, in addition to the noises that regulate each single graph. In what follows, we first briefly review PANDA in the single graph setting, and its regularization effects and theoretical properties in Sec 2.1. We then propose PANDA-JGL and PANDA-JFR for constructing multiple GGMs and UGMs in the NS framework in Sec 2.2, and extends PANDA-JGL and PANDA-JFR beyond the graphical models. For multiple GGMs, we also provide PANDA-CD and PANDA-SCIO with both the JGL and the JFR regularization in Sec 2.4.2 and 2.4.3, respectively, in addition to the PANDA-NS framework (Sec 2.4.1). The Bayesian interpretation is provided in Section 2.5.

### 2.1 PANDA for single graph estimation

PANDA is a noise augmentation, or broadly speaking, a noise injection (NI), originally proposed for regularizing GLMs and single UGM estimation. NI techniques, including adding or multiplying noises directly onto data (the data matrix remain its original dimension  $n \times p$ ) and attaching a noise matrix on to data matrix (either  $n$  or  $p$  are augmented), are effective in promoting generalization abilities of machine learning methods and simple in algorithm design. The learning process in NI is realized through iterative algorithms with adaptive independent noises injected in each iteration.

When employed to regularize single graphs, PANDA offers several choices on noise generating distributions (NGDs), each leading to a different type of regularization effects. Table 1 lists several example of the augmented noise type (see Li et al. (2018) for a more complete list). In the

noise type	NGD ( $k \neq j$ )	regularization effect $P(\Theta)$
bridge	$e_{jk} \sim N(0, \lambda  \theta_{jk} ^{-\gamma})$	$(\lambda n_e) \sum_{j=1}^p \sum_{j \neq k}  \theta_{jk} ^{2-\gamma}$
elastic-net	$e_{jk} \sim N(0, \lambda  \theta_{jk} ^{-1} + \sigma^2)$	$(\lambda n_e) \sum_{j=1}^p \sum_{j \neq k}  \theta_{jk}  + (\sigma^2 n_e) \sum_{j=1}^p \sum_{j \neq k} \theta_{jk}^2$
adaptive lasso	$e_{jk} \sim N(0, \lambda  \theta_{jk} ^{-1}  \hat{\theta}_{jk} ^{-\gamma})$	$(\lambda n_e) \sum_{j=1}^p \sum_{j \neq k}  \theta_{jk}   \hat{\theta}_{jk} ^{-\gamma}$

$\gamma \in (0, 2]; \lambda > 0; \sigma^2 > 0$  are tuning parameters.  $\hat{\theta}_{jk}$  in adaptive lasso is a consistent estimate for  $\theta_{jk}$ .  
PANDA can also yield SCAD, group lasso, fused ridge types of regularization; see Li et al. (2018)

Table 1: PANDA regularization noises and the corresponding regularization effects

regression-based NS approach,  $e_{jk}$  denotes the augmented data to covariate node  $X_k$  with the outcome node  $X_j$ . The augmented data to outcome  $X_j$  vary by its types. If  $X_j$  is Gaussian conditional on  $\mathbf{X}_j$ , then  $e_{jj} = 0$ ; when  $X_j$  is conditionally Poisson, Exponential, Bernoulli (with the  $(-1, 1)$  coding), and negative binomial (NB); then  $e_{jj} = 1$ .  $\theta_{jk}$  is the regression coefficient associated with  $X_j$ . If  $\theta_{jk}$  is not 0, then there is no edge between nodes  $k$  and  $j$ . When PANDA is used for estimating MGMs where node  $j$  and  $k$  are of different types (e.g. Gaussian vs Bernoulli), due to the asymmetry in the regressions on  $X_j$  and  $X_k$ ,  $\theta_{jk}$  and  $\theta_{kj}$  would have different interpretation from a regression perspective. However, the actual magnitude or interpretation would not be important if the goal is to decide there are edges or not. In the PANDA algorithm, a threshold  $\tau_0$  is often pre-specified for setting  $\hat{\theta}_{jk} = \hat{\theta}_{kj} = 0$ . When  $|\hat{\theta}_{jk} \hat{\theta}_{kj}| < \tau_0$ , then there is no edge; when  $\hat{\theta}_{jk} \hat{\theta}_{kj} > \tau_0$ ,  $\min\{\hat{\theta}_{jk}, \hat{\theta}_{kj}\}$  can be used an estimate for the edge weight (other approaches can also be used, such as the mean or the geometric mean).

The regularization effects listed in Table 1 is the penalty term on  $\Theta$  in the penalized loss function, by taking the expectation of the loss function given the augmented data over the distribution of the

augmented noise. In practice, this expectation can be obtained by letting  $n_e \rightarrow \infty$  while keeping  $\lambda n_e \sim O(1)$  (similar for  $\sigma^2 n_e$  in the elastic-net case) in one iteration of the PANDA algorithm, or by taking the average of noise-augmented loss functions from  $m \rightarrow \infty$  consecutive iterations. In the former case,  $(\lambda n_e)$  or  $\sigma^2 n_e$  is treated as one tuning parameter. It should be noted that, except for in the GGM case, letting  $n_e \rightarrow \infty$  would achieve the designed regularization effect arbitrarily well, while letting  $m \rightarrow \infty$  would give the second-order approximate regularization effect; however, the differences are negligible unless  $|\theta|$  is large (Li et al., 2018).

In the case of GGMs specifically, in addition to the NS approach, PANDA can also construct the GGM through the Cholesky decomposition (CD) of the precision matrix, through the SCIO estimator, through regularization of partial correlation coefficients to identify the hub nodes as in the SPACE approach (Peng et al., 2009), and through regularizing the precision matrix as a whole with the graphical ridge penalty.

## 2.2 PANDA-NS for simultaneous construction of multiple UGMs

Both of the two PANDA extensions we propose for the simultaneous multiple graph estimation employ the NS framework and perform node-wise GLM regression on the combined noise-augmented data across multiple graphs, assuming the nodes, say node  $X_j$  ( $j = 1, \dots, p$ ) in the same position across the  $q$  graphs is of the same type and its conditional distribution given all other nodes  $\mathbf{X}_{-j}$  in the same graph can be modelled via the Exponential family

$$p(X_j | \mathbf{X}_{-j}) = \exp(X_j \eta_j - B_j(\eta_j) + h_j(X_j)), \quad (1)$$

where  $\mathbf{X}_{-j} = (X_1, \dots, X_{j-1}, X_{j+1}, \dots, X_p)^T$ , and  $\eta_j$  is the natural parameter. In the GLM framework,  $\eta_j = \sum_{k \neq j} \theta_{jk} X_k$ . If the canonical link function  $g_j$  is used (e.g., the identity link for Gaussian  $X_j$  and the logit link for Bernoulli  $X_j$ ). If the  $\theta_{jk} = 0$  from the GLM with outcome node  $X_j$  or  $\theta_{kj} = 0$  from the GLM with outcome node  $X_k$ , then there is no edge between nodes  $j$  and  $k$ ; otherwise, the two nodes are connected with an edge. Yang et al. (2014, 2015a) proved that asymptotically with probability 1 that the neighborhood structure of conditionally exponential family graphical models can be recovered exactly.

We employ two types of noises in the simultaneous multiple graph construction. The first type of noise, denoted by  $e_1$ , regularizes the estimation of each graph and can be generated from any NDG in Table 1. For example, if the bridge-type noises are to be used, then

$$e_{ijk,1}^{(l)} \stackrel{\text{ind}}{\sim} N\left(0, \lambda_1^{(l)} |\theta_{jk}^{(l)}|^{-\gamma}\right) \quad (2)$$

for  $i = 1, \dots, n_{e_1}$ , where  $\lambda_1^{(l)}$  are the graph-specific tuning parameter. The second type of noise, denoted by  $e_2$ , achieves either the joint group lasso (JGL) or joint fused ridge (JFR) regularization on the edges in the position across the graphs. The JGL regularization, with augmented noise generated from Eqn (3), promotes structural similarity among the  $q$  graphs by placing the group lasso penalty on the  $q$   $\theta_{jk}^{(l)}$  values ( $l = 1, \dots, q$ ); while the JFR regularization, with augmented noise generated from Eqn (4), promotes the numerical similarity by placing the fused ridge penalty on the  $q$   $\theta_{jk}^{(l)}$  values.

$$\text{JGL: } e_{ijk,2}^{(l)} \stackrel{\text{ind}}{\sim} N\left(0, \lambda_2 \left(\sum_{l=1}^q \theta_{jk}^{2(l)}\right)^{-1/2}\right) \text{ for } k \neq j \quad (3)$$

$$\text{JFR: } \left(e_{ijk,2}^{(1)}, \dots, e_{ijk,2}^{(q)}\right) \stackrel{\text{ind}}{\sim} N\left(0, \lambda_2 (\mathbf{T}\mathbf{T}^T)\right) \text{ for } k \neq j \quad (4)$$

where the entries  $T_{kk} = 1, T_{k+1-k,1(k=q),k} = -1$  for  $k = 1, \dots, q$ ; and 0 otherwise. The values

of the augmented noisy data  $e_{jj,1}$  and  $e_{jj,2}$  for outcome node  $X_j$  depends on the node type as outlined in Li et al. (2018). Specifically,  $e_{jj,1} = e_{jj,2} \equiv 0$  for Gaussian  $X_j$ , and  $e_{jj,1} = e_{jj,2} \equiv 1$  for Bernoulli, Poisson, Exponential, and negative binomial nodes.

A fused lasso type of regularization can be obtained by using  $|\theta_k - \theta_{k'}|^{-1}$  ( $k \neq k'$ ) in the covariance matrix of  $\mathbf{e}$ ; however, it does not outperform the fused ridge in terms of promoting similarity on parameter estimation (or similarity on edge patterns when jointly estimating multiple graphs). Therefore we focus our discussion on the fused ridge through the rest of the paper.

Once the noisy data  $\mathbf{e}_1$  of size  $n_{e,1}$  and  $\mathbf{e}_2$  of  $n_{e,2}$  are generated, they will be tagged onto the observed data as illustrated in Figure 1. The figure uses  $q = 3$  graphs as an example, and the data augmentation scheme for any  $g \geq 2$  is similar.

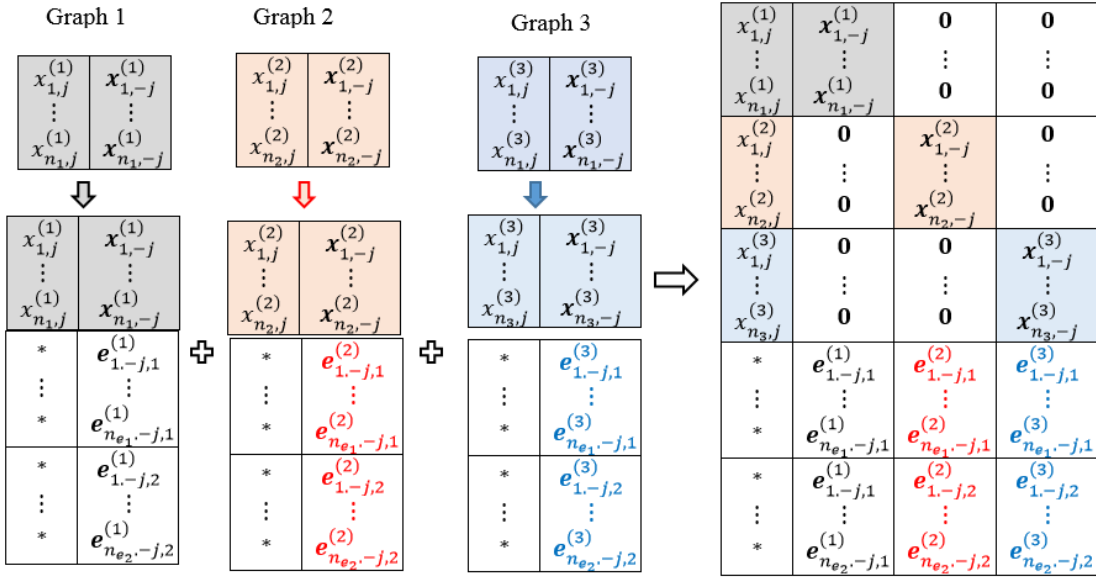


Figure 1: A schematic of data augmentation for three graphs in PANDA-JGL and PANDA-JFR (noise \* augmented to the outcome nodes  $X_j$  depends on the node type)

The summed negative log-likelihood function over  $p$  GLMs and  $q$  graphs on the combined noise-augmented data in one iteration is given by

$$l_p(\Theta|\mathbf{x}, \mathbf{e}_1, \mathbf{e}_2) = l(\Theta|\mathbf{x}) + l(\Theta|\mathbf{e}), \quad \text{where} \quad (5)$$

$$l(\Theta|\mathbf{e}) = -\sum_{l=1}^q \sum_{j=1}^p \sum_{h=1}^2 \sum_{i=1}^{n_{e,h}} \left( h_j \left( e_{ij,h}^{(l)} \right) + \sum_{k \neq j} \left( \theta_{jk}^{(l)} e_{ijk,h}^{(l)} \right) e_{ij,h}^{(l)} - B_j \left( \eta_{ij,h}^{(l)} \right) \right),$$

and  $\eta_{ij,h}^{(l)} = \sum_{k \neq j} \theta_{jk}^{(l)} e_{ijk,h}^{(l)}$  when the canonical link is used in the GLM. Proposition 1 shows the regularization effects of PANDA-NS-JGL and PANDA-NS-JFR in joint estimating multiple UGMs using the bridge-type noise  $e_1$  as an example. The proof is provided in Appendix B. The expected regularization effect can be easily obtained for other types of  $e_1$  noise with the only the difference in the formulation of the  $P_1$  term below.

**Proposition 1 (Regularization effects of PANDA-JGL and PANDA-JFR for multiple UGMs).** *The expectation of the second-order approximation of  $l_p(\Theta|\mathbf{x}, \mathbf{e})$  in Eqn (5) over the distribution of  $\mathbf{e}_1$  in Eqn (2) and  $\mathbf{e}_2$  in Eqn (3) or Eqn (4) is*

$$E_{\mathbf{e}}(l_p(\Theta|\mathbf{x}, \mathbf{e}_1, \mathbf{e}_2)) \approx l(\Theta|\mathbf{x}) + P_1 \left( n_{e,1}, \lambda_1^{(l)}, \Theta \right) + P_2 \left( n_{e,2}, \lambda_2, \Theta \right) + C + n_e O \left( \sum_{j=1}^p \theta_j^4 \cdot E(\mathbf{e}_j^4) \right)$$



$$\begin{aligned}
P_1(n_{e,1}\lambda_1^{(l)}, \Theta) &= \frac{n_{e,1}}{2} \sum_{l=1}^q \sum_{j=1}^p \sum_{k \neq j} \left( \theta_{jk}^{2(l)} V(e_{ijk,1}^{(l)}) \frac{\partial^2}{\partial e_{ijk,1}^2} l(\Theta|\mathbf{e})|_{e_{ijk,1}^{(l)}=0} \right), \\
P_2(n_{e,2}, \lambda_2, \Theta) &= \\
&\begin{cases} \frac{n_{e,2}}{2} \sum_{l=1}^q \sum_{j=1}^p \sum_{k \neq j} \left( \theta_{jk}^{2(l)} V(e_{ijk,2}^{(l)}) \frac{\partial^2}{\partial e_{ijk,2}^2} l(\Theta|\mathbf{e})|_{\mathbf{e}_1=0} \right) & \text{for JGL} \\ \frac{n_{e,2}}{2} \sum_{j=1}^p \sum_{k \neq j} \left[ \sum_{l=1}^q \theta_{jk}^{2(l)} V(e_{ijk,2}^{(l)}) \frac{\partial^2}{\partial e_{ijk,2}^{(l)2}} l(\Theta|\mathbf{e})|_{\mathbf{e}_2=0} \right. \\ \quad \left. - \sum_{l=1}^q \sum_{v=l-1} \theta_{jk}^{(l)} \theta_{jk}^{(v)} E(e_{ijk,2}^{(l)} e_{ijk,2}^{(v)}) \frac{\partial^2}{\partial e_{ijk,2}^{(l)} \partial e_{ijk,2}^{(v)}} l(\Theta|\mathbf{e})|_{\mathbf{e}_2=0} \right] & \text{for JFR,} \end{cases} \\
n_e &= n_{e,1} + n_{e,2} \text{ and } C \text{ is a known constant that relates to } n_{e,1}, n_{e,2} \text{ and } p.
\end{aligned}$$

When a node conditional on other nodes can be modelled with any of the following distributions: {Gaussian, Bernoulli, Exponential, Poisson}, then

$$P_1(n_{e,1}, \lambda_1^{(l)}, \Theta) = \frac{n_e}{2} l''(\Theta|\mathbf{0}) \sum_{l=1}^q \sum_{j=1}^p \sum_{k \neq j} \theta_{jk}^{2(l)} V(e_{ijk,1}^{(l)}), \quad (6)$$

$$P_2(n_{e,2}, \lambda_2^{(l)}, \Theta) = \begin{cases} \frac{\lambda_2 n_e}{2} l''(\Theta|\mathbf{0}) \sum_{j=1}^p \sum_{k \neq j} \left( \sum_{l=1}^q \theta_{jk}^{2(l)} \right)^{1/2} & \text{for JGL} \\ \frac{\lambda_2 n_e}{2} l''(\Theta|\mathbf{0}) \sum_{j=1}^p \sum_{k \neq j} \sum_{l=1}^q \sum_{v=l-1} \left( \theta_{jk}^{(l)} - \theta_{jk}^{(v)} \right)^2 & \text{for JFR,} \end{cases} \quad (7)$$

and  $C = 0$  of Gaussian,  $C = \log(2)pN$  for Bernoulli,  $C = pN$  for Exponential,  $C = 2pN$  for Poisson nodes, and  $C = (r+1)\log(r)pN$  for NB nodes ( $r$  is the number of failures), respectively, where  $N$  is a function of  $n_{e,1}, n_{e,2}, p$  that doesn't involve unknown parameters  $\Theta$ .

Operationally, the model parameters  $\Theta$  are estimated through running  $p$  GLMs on the noised augmented data combined across the  $q$  graphs, one per node, in an iterative fashion. The algorithmic steps are listed in Algorithm 1. Most of the remarks on the specification of the algorithmic parameters for the PANDA algorithms in single graph estimation in Li et al. (2018) apply directly to the multiple graph case, which are summarized in Remark 1. The only additional consideration is the relative sizes on  $n_{e,1}$  and  $n_{e,2}$ , as presented in Remark 2.

**Remark 1 (Algorithmic Parameters specification).** *Maximum iteration  $T$  is set at a relatively large value ( $T = O(10)$ ) so as for the algorithm to meet convergence criteria, including whether the trace plot of  $\bar{l}^t$  is fluctuating around a fixed level, whether the percentage change has fall below a threshold  $|\bar{l}^{(t+1)} - \bar{l}^{(t)}|/\bar{l}^{(t)} < \tau$  and whether  $\bar{l}^{(t)}$  is statistically tested to have converged (provided in Sec. 4.4 (Li et al., 2018)). Threshold  $\tau_0$  is set at a small value to set non-significant parameters estimates to 0, which is necessary and reasonable in that with  $n_e \rightarrow \infty$ , there exist a diminishing fluctuation in parameter estimations per iteration. A large  $n_{e,1}, n_{e,2}$  or  $m$  is needed to obtain the expected regularization effects, the former provides arbitrarily well second order Taylor approximated expected regularization, while the later is fast in computation.*

**Remark 2 (Choice of  $n_{e,1}$  and  $n_{e,2}$ ).** *First,  $\sum_{l=1}^1 n_1 + n_{e,1} + n_{e,2} > 3p$  so that the MLE can be solved uniquely in each regression at each iteration.  $n_{e,1}$  relates to the amount of regularization effect on single graph estimation, while  $n_{e,2}$  relates to the amount of imposed similarity in structures across multiple graphs. Though these two values can be specified independently, they are somewhat related. For example, if  $n_{e,1}\lambda_1$  is large if the lasso-type of noises is used, then each individual graph would be sparse to start with, and the graphs may be already similar enough even if  $n_{e,2}\lambda_2$  is not large. On the other hand. If the single graphs are still dense after proper tuning  $n_{e,1}\lambda_1$ , and if it believed that the dense structure would remain roughly the same across graph except for a few alterations, then  $n_{e,2}\lambda_2$  would be set a large value to promote the structural similarity. The graphical methods in Danaher et al. (2014) are in a similar situation, and they do not have "an theoretically optimal value" for the parameters that controls the relative separate vs. simultaneous*

---

**Algorithm 1** PANDA-NS-JGL and PANDA-NS-JFG for joint estimation of  $q$  UGMs
 

---

1: **Input:**

- random initial estimates  $\bar{\theta}_j^{(l)(0)}$  for  $j = 1, \dots, p$  and  $l = 1, \dots, q$ .
- a NGD for generating  $e_1$  with proper tuning parameters (Table 1), a NGD for  $e_2$  with proper tuning parameters (Eqn (3) for PANDA-JGL and Eqn (4) for PANDA-JFR), maximum iteration  $T$ , noisy data sizes  $n_{e,1}$  and  $n_{e,2}$ , threshold  $\tau_0$ , width of moving average (MA) window  $m$ , banked parameter estimates after convergence  $r$ .

2:  $t \leftarrow 0$ ; convergence  $\leftarrow 0$

3: **WHILE**  $t < T$  **AND** convergence = 0

4:   **FOR**  $j = 1 : p$

- a) Generate  $e_{ijk,1}^{(l)}$  for  $i = 1, \dots, n_{e,1}$ , and  $e_{ijk,2}^{(l)}$  for  $i = 1, \dots, n_{e,2}$ , with  $\bar{\theta}_j^{(l)(t-1)}$  plugged in the variance terms of the NGDs.
- b) Obtain augmented data  $\tilde{\mathbf{x}}$  by combining the original data  $\mathbf{x}$  with  $\mathbf{e}_1$  and  $\mathbf{e}_2$  in a similar manner as in Figure 1.
- c) Run GLM with outcome node  $\tilde{\mathbf{x}}_j$  with the a proper link function and linear predictor  $\tilde{\mathbf{x}}_{-j}^{(1)}\theta_j^{(1)} + \tilde{\mathbf{x}}_{-j}^{(2)}\theta_j^{(2)} + \dots + \tilde{\mathbf{x}}_{-j}^{(q)}\theta_j^{(q)}$  to obtain the MLE  $\hat{\theta}_j^{(l)(t)}$  for  $l = 1, 2, \dots, q$ .
- d) If  $t > m$ , calculate the MA  $\bar{\theta}_j^{(l)(t)} = m^{-1} \sum_{b=t-m+1}^t \hat{\theta}_j^{(l)(b)}$ ; otherwise  $\bar{\theta}_j^{(l)(t)} = \hat{\theta}_j^{(l)(t)}$  for  $l = 1, \dots, q$ .

**End FOR**

5:   Plug in  $\bar{\theta}_j^{(l)(t)}$  in Eqn (5) to calculate the overall loss function and apply one of the convergence

6:   criteria from Li et al. (2018) to  $\bar{l}^{(t)}$ . Let convergence  $\leftarrow 1$  if the convergence is reached.

7:   **End WHILE**

8: Continue to execute the command lines 4 and 6 for another  $r$  iterations, and record  $\bar{\theta}_j^{(l)(b)}$  for  $b = t + 1, \dots, t + r$  and  $l = 1, \dots, q$ . Let  $\bar{\theta}_{jk}^{(l)} = (\bar{\theta}_{jk}^{(l)(t+1)}, \dots, \bar{\theta}_{jk}^{(l)(t+r)})$ .

9: Set  $\hat{\theta}_{jk}^{(l)} = \hat{\theta}_{kj}^{(l)} = 0$  if  $\left( |\max\{\bar{\theta}_{jk}^{(l)}\} \cdot \min\{\bar{\theta}_{jk}^{(l)}\}| < \tau_0 \right) \cap \left( \max\{\bar{\theta}_{jk}^{(l)}\} \cdot \min\{\bar{\theta}_{jk}^{(l)}\} < 0 \right)$  or  $\left( |\max\{\bar{\theta}_{kj}^{(l)}\} \cdot \min\{\bar{\theta}_{kj}^{(l)}\}| < \tau_0 \right) \cap \left( \max\{\bar{\theta}_{kj}^{(l)}\} \cdot \min\{\bar{\theta}_{kj}^{(l)}\} < 0 \right)$ ;  $\hat{\theta}_{jk}^{(l)} = \hat{\theta}_{kj}^{(l)} = \min\{\bar{\theta}_{jk}^{(l)}, \bar{\theta}_{kj}^{(l)}\}$  otherwise.

10: **Output:**  $\hat{\theta}^{(1)}, \dots, \hat{\theta}^{(q)}$ .

---

regularization across graphs as “the optimal value would need to be a function of the number of covariates and group sizes among other things”. Finally, while  $n_{e,1}^{(l)}, n_{e,2}^{(l)}$  may vary by graph, it is not necessary as it yields no difference in the expected regularization effect from using the same  $n_{e,1}$  and  $n_{e,2}$  across graph. In addition, the augmented data can no longer be combined in the same way as in Figure 1; but rather the noisy data should be tagged onto the observed data  $\mathbf{x}$  in a similar diagonal manner as how  $\mathbf{x}^{(l)}$  are combined for  $l = 1, \dots, q$  in Figure 1.

### 2.3 PANDA-JGL and PANDA-JFR beyond graphical models

The JGL and JFR regularization via PANDA can be generalized beyond the graphical model estimation to regularize the variable selection and parameter estimation in GLMs in general. Specifically, used in the regression framework, the JGL regularization is equivalent to the sparse group lasso (SGL) regularization (Simon et al., 2013), where the group lasso penalty will be imposed on a group of variables that will be selected in an all-or-none manner per regularization.

We propose the *sparse fused ridge (SFR)* regularization as a counterpart to the JFR regularization beyond the graphical model estimation, where the fused ridge penalty is applied to the variables belonging to the same group to promote the numerical similarity among their associated regression coefficients. Similar to the SGL to JGL, the SFR is the expected regularization to JFR with respect to the distribution of augmented noise. In the regression setting, SFR is not inferior to sparse



fused lasso (SFL) (Tibshirani et al., 2005) in terms of simultaneously promoting sparsity across groups and similarity within groups, while enjoying a simpler formulation in PANDA. Specifically, the variance of the augmented noise in PANDA with the JFR/SFR regularization as given in Eqn 4 does not involve the parameters under regularization and does not change with iteration  $t$ , while with SFL, the variance of the noise terms is a function of the parameters  $|\theta_{jk}^{(l)} - \theta_{jk}^{(v)}|^{-1}$  ( $l \neq v$ ), which is constantly being updated with the parameter estimates from the latest iteration of the PANDA algorithm. In addition, the JFR/SFR regularization has a corresponding Bayesian prior in the Bayesian hierarchical modelling framework, as we prosed in Sec 2.5, while there does not appear to an obvious Bayesian counterpart to the JFR/SFR regularization.

## 2.4 PANDA for simultaneous construction of multiple GGMs

GGMs are a special type of UGMs when all the nodes can be modelled using a Gaussian distribution given the other nodes in the same graph, and every GGM can be reformulated a multivariate Gaussian distribution (MGD) mathematically. Leveraging this connection between the graph structure and the precision matrix of the MGD, there are multiple approaches to construct the GGMs simultaneously. We list three of these approaches, the NS method included, and show PANDA can realize them through noise augmentation.

### 2.4.1 PANDA-NS for multiple GGMs estimation

For GGMs, the augmented noise to outcome  $X_j$  is  $e_{jj,1} = e_{jj,2} \equiv 0$ . As for the augmented noise to the covariate node  $X_k$ ,  $e_{jk,1}^{(l)}$  ( $k \neq j$ ) is independently generated for each graph  $l = 1, \dots, q$  from a NGD in Table 1;  $e_{jk,2}^{(l)}$  can be generated from Eqns (3) or (4), depending on the desired similarity- promoting regularization.

Algorithm 1 applies directly to the GGM case, with a few modifications tailored for the GGMs. First, We would standardize the raw data  $\mathbf{x}^{(l)}$  for  $l = 1, \dots, q$  as a pre-processing step and used the standardized  $\mathbf{x}^{(l)}$  in all later steps. Second, with the Gaussian nodes, we could just run linear regression to obtain the OLS estimator at each iteration. Third, the loss function used in the stopping criterion is the summed SSE across the  $p$  regressions  $\sum_{j=1}^p \text{SSE}_j$  with the noise augmented data in Eqn (8), where  $\Theta = (\Theta^{(1)}, \dots, \Theta^{(q)})$  contain all the regression parameters,  $\mathbf{x} = (\mathbf{x}^{(1)}, \dots, \mathbf{x}^{(q)})$ , and  $\mathbf{e}_1 = (\mathbf{e}_1^{(1)}, \dots, \mathbf{e}_1^{(q)})$ , and  $\mathbf{e}_2 = (\mathbf{e}_2^{(1)}, \dots, \mathbf{e}_2^{(q)})$ .

$$l_p(\Theta|\mathbf{x}, \mathbf{e}_1, \mathbf{e}_2) = \sum_{l=1}^q \sum_{i=1}^{n_l} \sum_{j=1}^p \left( x_{ij}^{(l)} - \sum_{k \neq j} x_{ik}^{(l)} \theta_{jk}^{(l)} \right)^2 + \sum_{h=1}^2 \sum_{i=1}^{n_{e,h}} \sum_{j=1}^p \left( e_{ijj,h} - \sum_{l=1}^q \sum_{j \neq k} e_{ijk,h}^{(l)} \theta_{jk}^{(l)} \right)^2. \quad (8)$$

Finally, the estimate  $\hat{\sigma}_j^2$  is given by  $\text{SSE}_j / (\sum_{l=1}^q n_l - \nu_j)$ , where  $\nu_j = \text{trace}(\mathbf{x}_j(\tilde{\mathbf{x}}_j' \tilde{\mathbf{x}}_j)^{-1} \mathbf{x}_j')$  is the degrees of freedom calculated as the trace of the hat matrix formulated with the noise-augmented data  $\tilde{\mathbf{x}}$ ; and the algorithm outputs  $\hat{\omega}_{jj} = \hat{\sigma}_j^{-2}$  and  $\hat{\Omega}_{-j,j}^{(l)} = -\hat{\boldsymbol{\theta}}_j^{(l)} \hat{\omega}_{jj}^{(l)}$ .

It is worth noting that the JGL regularization on  $\theta_{jk}$  can also be derived by formulating the NGD for  $e_2$  with the entries  $\omega_{jk}$  of the precision matrix  $\Omega$ , given the relationship  $\theta_{kj} = -\omega_{jj}^{-1} \omega_{kj}$ . Specifically,  $e_{ijk,2}^{(l)} \stackrel{\text{ind}}{\sim} N\left(0, \lambda_2 \left(\sum_{l=1}^q (\omega_{jk}^{(l)})^2\right)^{-\frac{1}{2}}\right)$ , which can be rewritten as  $N\left(0, \lambda_2 \omega_{jj}^{(l)} \left(\sum_{l=1}^q (\theta_{jk}^{(l)})^2\right)^{-\frac{1}{2}}\right)$  since  $\sum_{l=1}^q (\omega_{jk}^{(l)})^2 = \sum_{l=1}^q (\omega_{jj}^{(l)})^{-2} (\theta_{jk}^{(l)})^2$ . In such a case,  $\omega_{jj}^{(l)}$  can be regarded as a nuisance parameter and be bundled together with  $\lambda$  as one tuning parameter  $\lambda$  and the regularization per se still occurs on  $\theta_{jk}$ . Furthermore,  $\omega_{jj}^{(l)}$  can be set the same across all  $q$  graphs, especially that

PANDA runs on one combined standardized data set across the  $q$  GGMs.

Corollary 1 is a special case of Proposition 1 and shows that PANDA-NS-JGL and PANDA-NS-JFR promote the structural or numerical similarity on the edges in the same position among graphs, respectively, in addition to the regularization on each graph charged through augmenting with  $\mathbf{e}_1$ . The proof is given in Appendix A. Corollary 1 is given in terms of the bridge-type noise on  $e_1$ . The expected regularization for other NGDs for  $\mathbf{e}_1$  takes similar forms as Eqns (9) and (10), with the first penalty term on  $\theta_j$  being replaced with the corresponding regularization effect associated with the corresponding NGD in Table 1.

**Corollary 1 (Regularization effect of PANDA-NS-JGL and PANDA-NS-JFR for multiple GGMs).** For  $\mathbf{e}_1$  drawn from Eqns (2) and  $\mathbf{e}_2$  drawn from Eqn (3) or (4), respectively, the expected noise-augmented loss function  $E_e(l_p(\Theta|\mathbf{x}, \mathbf{e}_1, \mathbf{e}_2))$  with regard to the distributions of  $\mathbf{e} = \{\mathbf{e}_1, \mathbf{e}_2\}$  is

$$JGL: l(\Theta|\mathbf{x}) + \sum_{l=1}^q \lambda_1^{(l)} n_{e,1} \sum_{j=1}^p \sum_{j \neq k} \left| \theta_{jk}^{(l)} \right|^{2-\gamma} + \sum_{j=1}^p \lambda_2 n_{e,2} \omega_{jj} \sum_{j \neq k} \left( \sum_{l=1}^q \theta_{jk}^{(l)} \right)^{1/2} \quad (9)$$

$$JRF: l(\Theta|\mathbf{x}) + \sum_{l=1}^q \lambda_1^{(l)} n_{e,1} \sum_{j=1}^p \sum_{j \neq k} \left| \theta_{jk}^{(l)} \right|^{2-\gamma} + \sum_{j=1}^p \lambda_2 n_{e,2} \omega_{jj}^2 \sum_{k \neq j} \sum_{l=1}^q \sum_{v=l-1} \left( \theta_{jk}^{(l)} - \theta_{jk}^{(v)} \right)^2 \quad (10)$$

#### 2.4.2 PANDA-CD for multiple GGMs estimation

The Cholesky decomposition (CD) approach refers to estimating the precision matrix through the LDL decomposition, a variant of the CD. Compared to the NS approach in Section 2.4.1, the CD approach guarantees symmetry and positive definiteness of the estimated precision matrix. WLOG, let  $\mathbf{x}_{n \times p}^{(l)} \sim N_p(\mathbf{0}, \Omega^{(l)})$ . The CD of  $\Omega$  is  $\Omega = L^T D^{-1} L$ , such that  $|\Omega| = |D|^{-1} = \prod_{j=1}^p \sigma_j^{-2}$ , where  $D = \text{diag}(\sigma_1^2, \dots, \sigma_p^2)$ , and  $L$  is a lower uni-triangular matrix with elements  $-\theta_{jk}$  for  $j > k$ , 0 for  $k < j$ , and 1 for  $j = k$ .

The parameters in GGM estimation through CD in graph  $l$  include the regression coefficients  $\Theta^{(l)}$  from a sequence of regression models and the variance terms  $\sigma^{2(l)}$  for  $l = 1, \dots, q$ . Specifically, Let  $L\mathbf{X} = \boldsymbol{\epsilon}$ , where  $\boldsymbol{\epsilon} \sim N(\mathbf{0}, D)$ . Then

$$X_1 = \epsilon_1 \text{ and } X_j = \sum_{k=1}^{j-1} X_k \theta_{jk} + \epsilon_j \text{ for } j = 2, \dots, p, \quad (11)$$

suggesting the following sequence of regression models:  $X_2$  regressed on  $X_1$ ,  $X_3$  regressed on  $(X_1, X_2)$ , and so on. Huang et al. (2006) apply the  $l_\gamma$  ( $\gamma > 0$ ) regularization in estimating  $\theta_{jk}$  and minimize it by solving Eqns (13) and (12) alternatively in an iterative manner.

$$\hat{\boldsymbol{\theta}}_j = \arg \min_{\boldsymbol{\theta}_j} \hat{\sigma}_j^{-2} \sum_{i=1}^n \left( \mathbf{x}_{ij} - \sum_{k=1}^{j-1} \mathbf{x}_{ik} \theta_{jk} \right)^2 + \xi \sum_{k=1}^{j-1} |\theta_{jk}|^\gamma. \quad (12)$$

$$\hat{\sigma}_j^2 = n^{-1} \sum_{i=1}^n \left( \mathbf{x}_{ij} - \sum_{k=1}^{j-1} \mathbf{x}_{ik} \hat{\boldsymbol{\theta}}_{jk} \right)^2, \quad (13)$$

Optimization and regularization occurs only on  $\boldsymbol{\theta}_j$  in Eqn (12), whereas  $\hat{\sigma}_j^2$  in Eqn (13) is given once  $\boldsymbol{\theta}_j$  is estimated. However, since Eqn (12) involves  $\hat{\sigma}_j^2$ , iterations alternatively estimating  $\hat{\sigma}_j^2$  and  $\boldsymbol{\theta}_j$  are needed.

Let  $\Theta = (\Theta^{(1)}, \dots, \Theta^{(q)})$ ,  $\boldsymbol{\sigma}^2 = (\sigma^{2(1)}, \dots, \sigma^{2(q)})$  across  $q$  GGMs. As in the NS case, PANDA offers the JGL and JFR regularization when simultaneously estimating the  $q$  GGMs through CD via augmenting two types of noise. The first type of noise  $\mathbf{e}_{i,1}$  can be chosen from any NDG in

Table 1. For example, if the bridge noise is used, then

$$e_{ijk,1}^{(l)} \stackrel{\text{ind}}{\sim} N\left(0, \lambda_1^{(l)} \sigma_j^{(l)2} |\theta_{jk}^{(l)}|^{-\gamma}\right); \text{ and } e_{ijj,1}^{(l)} = 0 \text{ for } i = 1, \dots, n_{e,1}. \quad (14)$$

Similar to the GGM-NS framework, we set  $\sigma_j^{(l)2}$  the same across  $q$  graphs. The second type of noise  $\mathbf{e}_{i,2}$  for  $i = 1, \dots, n_{e,2}$  is drawn from Eqns (15) and (16) to achieve the JGL and the JFR regularization, respectively, in the CD framework

$$\text{JGL: } e_{ijk,2}^{(l)} \stackrel{\text{ind}}{\sim} N\left(0, \lambda_2 \sigma_j^2 \left(\sum_{l=1}^q \theta_{jk}^{2(l)}\right)^{-1/2}\right) \text{ for } k < j; \text{ and } e_{ijj,2}^{(l)} = 0. \quad (15)$$

$$\text{JFR: } \left(e_{ijk,2}^{(1)}, \dots, e_{ijk,2}^{(q)}\right) \stackrel{\text{ind}}{\sim} N\left(0, \lambda_2 \sigma_j^2 (\mathbf{T}\mathbf{T}^T)\right) \text{ for } k < j; \text{ and } e_{ijj,2}^{(l)} = 0, \quad (16)$$

where  $T_{kk} = 1, T_{k+1-k-1(k=q),k} = -1$  for  $k = 1, \dots, q$ ; and 0 otherwise.

The way to augment data in the CD setting is similar in the NS setting in Figures 1, except that the covariate node dimension grows with  $j$ . An example on how the augmented noises are tagged onto the observed data for PANDA-JGL and -JFR in the CD setting is presented in Figure 2. Note that when  $j = 1$ , there are no covariate nodes or regression models, the augmented  $\tilde{\mathbf{x}}_1$  (the first column in the combined augmented data) is used to estimate  $\sigma_1^2$ . The algorithmic steps,

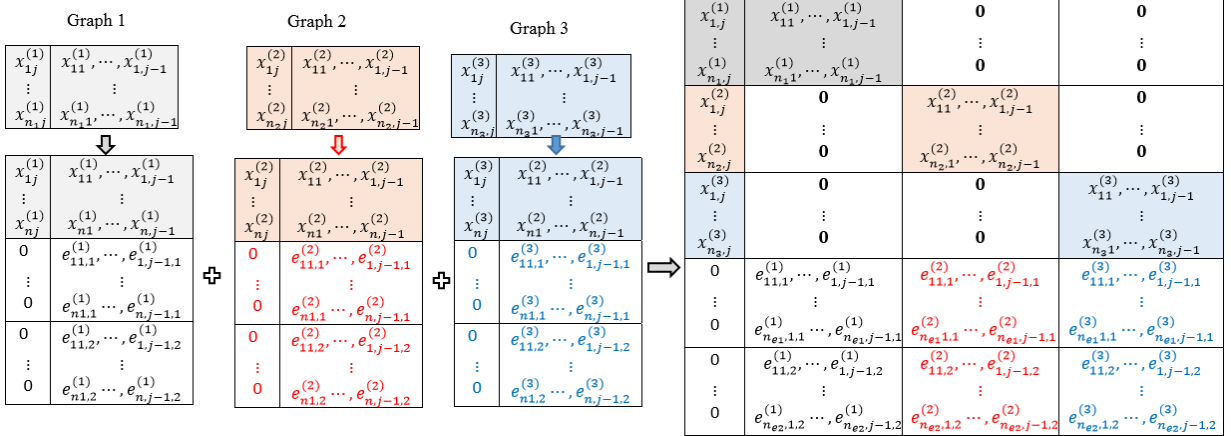


Figure 2: A schematic of data augmentation in PANDA-JGL and -JFR for CD for three GGMS. When  $j = 1$ , there are no covariate nodes or regression models, the augmented  $\tilde{\mathbf{x}}_1$  (the first column in the combined augmented data) is used to estimate  $\sigma_1^2$ .

available in Algorithm S1 in the Supplementary Materials, for implementing PANDA-JGL and PANDA-JFG for CD are similar to Algorithm 1, except that 1) the  $p$  linear regression models in the NS setting are replaced by  $p - 1$  regressions; 2) an additional inner loop is added within each regression at each iteration to alternatively solve for  $\Theta$  and  $\sigma$  as given in Eqns (12) and (13).

**Proposition 2 (PANDA-CD with JGL and -JFR regularization in Multiple GGMS).** *The noise-augmented loss function across the  $q$  graphs is*

$$l_p(\Theta|\mathbf{x}, \mathbf{e}_1, \mathbf{e}_2) = \sum_{l=1}^q \sum_{i=1}^{n_l} \sum_{j=1}^p \sigma_j^{-2} \left( x_{ij}^{(l)} - \sum_{k=1}^{j-1} x_{ik}^{(l)} \theta_{jk}^{(l)} \right)^2 + \sum_{h=1}^2 \sum_{i=1}^{n_{e,h}} \sum_{j=1}^p \sigma_j^{-2} \left( e_{ijj,h} - \sum_{l=1}^q \sum_{k=1}^{j-1} e_{ijk,h}^{(l)} \theta_{jk}^{(l)} \right)^2,$$

the expectation of which w.r.t. the distribution of  $\mathbf{e}_1$  and  $\mathbf{e}_2$ ,  $E(l_p(\Theta|\mathbf{x}, \mathbf{e}_1, \mathbf{e}_2)) =$

$$\text{JGL: } l(\Theta|\mathbf{x}) + \sum_{l=1}^q \lambda_1^{(l)} n_{e,1} \sum_{j=1}^p \sum_{k=1}^{j-1} |\theta_{jk}^{(l)}|^{2-\gamma} + \lambda_2 n_{e,2} \sum_{j=1}^p \sum_{k=1}^{j-1} \left( \sum_{l=1}^q \theta_{jk}^{2(l)} \right)^{1/2} \quad (17)$$

$$JFR: l(\Theta|\mathbf{x}) + \sum_{l=1}^q \lambda_1^{(l)} n_{e,1} \sum_{j=1}^p \sum_{k=1}^{j-1} \left| \theta_{jk}^{(l)} \right|^{2-\gamma} + \lambda_2 n_{e,2} \sum_{j=1}^p \sum_{k=1}^{j-1} \sum_{l=1}^q \sum_{v=l-1}^q \left( \theta_{jk}^{(l)} - \theta_{jk}^{(v)} \right)^2 \quad (18)$$

The expected loss functions in Eqn (17) and (18) suggest PANDA-JGL and PANDA-JFR impose either the group-lasso penalty across multiple graphs on the same parameter to promote structural similarity, or a fused-ridge penalty to promote structural pairwise numerical similarity, in addition to the (sparsity) regularization on the parameters in each of the single graphs. The proofs of Eqn (17) and (18) are similar to Appendix A.

### 2.4.3 PANDA-SCIO for multiple GGMs estimation

Let  $\theta_j$  be the  $j$ -th column of the precision matrix  $\Omega$  in a GGM. Liu and Xi (2015) propose the SCIO estimator which solves the following quadratic optimization problem:

$$\hat{\theta}_j = \arg \min_{\theta_j \in \mathbb{R}^p} \left\{ (2n)^{-1} \theta_j^t \mathbf{x}^T \mathbf{x} \theta_j - \mathbf{1}_j \theta_j + \lambda \sum_{k \neq j} |\theta_{jk}| \right\} \text{ separately for } j = 1, \dots, p. \quad \text{Li et al.}$$

(2018) provide a PANDA counterpart to SCIO in the single graph setting and simplify the problem to calculating  $\hat{\theta}_j = n (\tilde{\mathbf{x}}^T \tilde{\mathbf{x}})^{-1} \mathbf{1}_j$ , where  $\tilde{\mathbf{x}}$  is the noise-augmented data and  $\mathbf{1}_j$  is the  $j^{\text{th}}$  column of the identity matrix  $I_p$ . In this section we extend PANDA-SCIO in the single GGM setting to multiple GGMs with either the JGL or the JFR regularization. The first type of noise  $\mathbf{e}_{i,1}$  can be drawn from any NGD in Table 1. For example, if the bridge-type of noise is used, then

$$e_{ijk,1}^{(l)} \stackrel{\text{ind}}{\sim} N \left( 0, \lambda_1^{(l)} \left| \theta_{jk}^{(l)} \right|^{-\gamma} \right); \text{ and } e_{ijj,1}^{(l)} = 0 \text{ for } i = 1, \dots, n_{e,1}. \quad (19)$$

The similarity-promoting noise  $\mathbf{e}_{i,2}$  for  $i = 1, \dots, n_{e,2}$  is drawn from Eqn (20) and (21) for the JGL and JFR regularization, respectively

$$\text{JGL: } e_{ijk,2}^{(l)} \stackrel{\text{ind}}{\sim} N \left( 0, \lambda_2 \left( \sum_{l=1}^q \theta_{jk}^{2(l)} \right)^{-1/2} \right) \text{ for } k \neq j; \text{ and } e_{ijj,2}^{(l)} = 0. \quad (20)$$

$$\text{JFR: } (e_{ijk,2}^{(1)}, \dots, e_{ijk,2}^{(q)}) \stackrel{\text{ind}}{\sim} N \left( 0, \lambda_2 (\mathbf{T}\mathbf{T}^T) \right) \text{ for } k \neq j; \text{ and } e_{ijj,2} = 0 \quad (21)$$

where  $T_{kk} = 1, T_{k+1-k,1(k=q),k} = -1$  for  $k = 1, \dots, q$ ; and 0 otherwise. Before the data augmentation, the noises generated from Eqns (19), (20) and (21) are scaled to obtain  $\sqrt{2n}\mathbf{e}_{j,1}^{(l)}$  and  $\sqrt{2n}\mathbf{e}_{j,2}^{(l)}$ , which are tagged onto the observed data  $\mathbf{x}$  in a similar fashion as in Figure 1. Proposition 3 establishes the regularization effects on  $\Omega$  with the proof given in Appendix C.

#### Proposition 3 (PANDA-SCIO with JGL and JFR regularization in Multiple GGMs).

Let  $[\ast//\ast]$  denote two matrices combined by row and  $[\ast||\ast]$  denote two matrices combined by column. Denote the joint regression parameters and noises for column  $j, j = 1, \dots, p$  by  $\Theta_j = [\theta_j^{(1)} // \dots // \theta_j^{(q)}]$ ,  $\mathbf{e}_{j,1} = [\mathbf{e}_{j,1}^{(1)} || \dots || \mathbf{e}_{j,1}^{(q)}]$ , and  $\mathbf{e}_{j,2} = [\mathbf{e}_{j,2}^{(1)} || \dots || \mathbf{e}_{j,2}^{(q)}]$ . Denote the observed data, the collections of all model parameters, and all augmented noises by  $\mathbf{x} = (\mathbf{x}^{(1)} || \dots || \mathbf{x}^{(q)})$ ,  $\Theta = (\Theta_1 || \dots || \Theta_p)$ ,  $\mathbf{e}_1 = (\mathbf{e}_{1,1} || \dots || \mathbf{e}_{p,1})$ , and  $\mathbf{e}_2 = (\mathbf{e}_{1,2} || \dots || \mathbf{e}_{p,2})$ . Let  $\mathbf{B}_j = [\mathbf{1}_j // \dots // \mathbf{1}_j]$ , where  $\mathbf{1}_j$  is the  $j^{\text{th}}$  column of the identity matrix  $I_p$ . The noise-augmented loss function and its expectation w.r.t. the distribution of  $\mathbf{e}$  are respectively

$$l_p(\Theta|\mathbf{x}, \mathbf{e}_1, \mathbf{e}_2) = \frac{1}{2n} \sum_{j=1}^p \Theta_j^T (\tilde{\mathbf{x}}_j^T \tilde{\mathbf{x}}_j) \Theta_j - \sum_{j=1}^p \Theta_j^T \mathbf{B}_j \quad (22)$$

$$E(l_p(\Theta|\mathbf{x}, \mathbf{e}_1, \mathbf{e}_2)) \quad (23)$$

$$= l(\Theta|\mathbf{x}) + \lambda_1^{(l)} n_{e,1} \sum_{j=1}^p \sum_{j \neq k}^q \sum_{l=1}^q \left| \theta_{jk}^{(l)} \right|^{2-\gamma} + \begin{cases} \lambda_2 n_{e,2} \sum_{j=1}^p \sum_{j \neq k} \left( \sum_{l=1}^q \theta_{jk}^{2(l)} \right)^{1/2} & \text{for JGL} \\ \lambda_2 n_{e,2} \sum_{j=1}^p \sum_{k \neq j} \sum_{l=1}^q \sum_{v=l-1} \left( \theta_{jk}^{(l)} - \theta_{jk}^{(v)} \right)^2 & \text{for JFR.} \end{cases}$$

The minimizer of Eqn (22) can be solved by taking its derivative and setting it to be 0, giving  $\hat{\Theta}_j = n \left( \tilde{\mathbf{x}}_j^T \tilde{\mathbf{x}}_j \right)^{-1} \mathbf{B}_j$ . Note the inverse of  $\left( \tilde{\mathbf{x}}_j^T \tilde{\mathbf{x}}_j \right)$  exists since the augmented data  $\tilde{\mathbf{x}}_j$  has a sample size larger than its feature dimensionality. Also noted is that  $E_e \left( \tilde{\mathbf{x}}_j^T \tilde{\mathbf{x}}_j \right)$  for the JGL case is a block-diagonal matrix given that the noises in different graphs are independent, further simplifying the solution to  $\hat{\Theta}_j^{(l)} = 2n \left( \tilde{\mathbf{x}}_j^{(l)T} \tilde{\mathbf{x}}_j^{(l)} \right)^{-1} \mathbf{1}_j, l = 1, \dots, q$ .

The algorithmic steps for carrying out PANDA-SCIO is given in Algorithm S2 in the supplementary materials.

## 2.5 Bayesian Interpretation

Both the PANDA techniques and Bayesian modeling imposes regularization by introducing endogenous information. Li et al. (2018) draw connections between the two paradigms from two aspects. First, the various regularization effects as realized by PANDA have counterpart priors on the model parameters through Bayesian hierarchical modeling. Second, the parameters estimates obtained by PANDA at every iterations can be seen as obtaining the maximum a posterior (MAP) estimate in an empirical-Bayes (EB)-like framework. This section also provides an EB interpretation for PANDA in the joint estimation of multiple graphical models, as well as the prior that lead to the JFR/SFR in the Bayesian hierarchical setting. We use the bridge-type noise for illustration purposes, which can be easily modified to accommodate other NGDs in Table 1.

In the NS framework for constructing  $q$  UGMs simultaneously, it is the multivariate Gaussian priors on  $\theta^{(l)}$  ( $l = 1, \dots, q$ ) in iteration ( $t + 1$ ) that eventually lead to the JGL and JFR penalty on the edges, as presented below. T

$$\text{GGM JGL: } \pi \left( \theta_{jk}^{(1)}, \dots, \theta_{jk}^{(q)} | \sigma_j^2 \right) \propto \prod_{l=1}^q \exp \left\{ - (2\sigma_j^2)^{-1} \left( \lambda_1^{(l)} \frac{\theta_{jk}^{(l)2}}{|\theta_{jk}^{(l)(t)}|^\gamma} + \lambda_2 \frac{\theta_{jk}^{(l)2}}{\|\theta_{jk}^{(t)}\|_2} \right) \right\} \quad (24)$$

$$\text{GGM JFR: } \pi \left( \theta_{jk}^{(1)}, \dots, \theta_{jk}^{(q)} | \sigma_j^2 \right) \propto \exp \left\{ - (2\sigma_j^2)^{-1} \left( \sum_{l=1}^q \lambda_1^{(l)} \frac{\theta_{jk}^{(l)2}}{|\theta_{jk}^{(l)(t)}|^\gamma} + \lambda_2 \theta_{jk}^{(t)T} (\mathbf{T}\mathbf{T}^T) \theta_{jk}^{(t)} \right) \right\} \quad (25)$$

$\pi(\sigma_j^2) \propto \sigma_j^{-2}$  in Eqns (24) and (25);

$$\text{UGM JGL: } \pi \left( \theta_{jk}^{(1)}, \dots, \theta_{jk}^{(q)} \right) \propto \prod_{l=1}^q \exp \left\{ -2^{-1} \left( \lambda_1^{(l)} \frac{\theta_{jk}^{(l)2}}{|\theta_{jk}^{(l)(t)}|^\gamma} + \lambda_2 \frac{\theta_{jk}^{(l)2}}{\|\theta_{jk}^{(t)}\|_2} \right) \right\} \quad (26)$$

$$\text{UGM JFR: } \pi \left( \theta_{jk}^{(1)}, \dots, \theta_{jk}^{(q)} \right) \propto \exp \left\{ -2^{-1} \left( \sum_{l=1}^q \lambda_1^{(l)} \frac{\theta_{jk}^{(l)2}}{|\theta_{jk}^{(l)(t)}|^\gamma} + \lambda_2 \theta_{jk}^{(t)T} (\mathbf{T}\mathbf{T}^T) \theta_{jk}^{(t)} \right) \right\}, \quad (27)$$

where the entries  $T_{kk} = 1, T_{k+1-k \cdot 1(k=q),k} = -1$  for  $k = 1, \dots, q$ ; and 0 otherwise. It is straightforward to observe that priors in Eqn (24) and (26) result in the JGL regularization, while why the priors in Eqn (25) and (27) yields the JFR regularization is less obvious. We provide the justification for the latter in Appendix D.

In the Bayesian hierarchical modeling framework, the JFR/SFR regularization can be realized by

imposing the following priors on the model parameters. The joint hierarchical prior for a group of  $(\theta_{jk}^{(1)}, \dots, \theta_{jk}^{(q)})$  can be formulate as follows,

$$\pi(\boldsymbol{\nu}) = \prod_{l=1}^q \lambda_1^{2(l)} \nu^{(l)} \exp\left(-\lambda^{2(l)} \nu^{(l)2}/2\right)$$

$$\pi\left(\theta_{jk}^{(1)}, \dots, \theta_{jk}^{(q)} | \boldsymbol{\nu}\right) \propto \exp\left\{-2^{-1} \left(\boldsymbol{\theta}_{jk}^{(t)T} (\mathbf{diag}(\nu^{(1)}, \dots, \nu^{(q)})^{-2} + \lambda_2 \mathbf{T}\mathbf{T}^T) \boldsymbol{\theta}_{jk}^{(t)}\right)\right\},$$

where the sparsity promoting prior is a hierarchically modeled Laplace prior, as a mixture of Gaussian and Rayleigh, while the similarity promoting prior is a multivariate Gaussian. Since the multivariate Gaussian prior has precision matrix of rank  $q - 1$ , for the SFR prior to be a proper distribution, we need  $\lambda_1^{(l)} > 0, l = 1, \dots, q$ .

Note that the JFL/SFL regularization cannot be easily formulated using a Bayes prior in the hierarchical modelling framework; see [Casella et al. \(2010\)](#).

### 3 Simulation

We applied PANDA-JGL and PANDA-JFR to jointly train three graphs in GGM and PGM. Since we could not locate any approaches for jointly estimating non-Gaussian UGMs, we compared PANDA with the naïve differencing approach, which constructs each graph separately and then compares the edge connection patterns in each pair of the estimated graphs in a post-hoc manner. For GGMs, there exist a couple of joint estimation approaches (see Section 1), to which PANDA was compared, including the joint graphical lasso approach with the group lasso (GL) penalty and the fused lasso (FL) penalty ([Danaher, 2013](#); [Danaher et al., 2014](#)), and the SGL regularization with the lasso and GL penalty (note the SGL is equivalent to the PANDA-NS-JGL in expectation). Among all the joint estimation approaches, only the two joint graphical lasso methods lead to positive definite precision estimates.

The simulation schemes are summarized in Table 2. For simplicity, we kept  $n$  the same across the 3 graphs. For each graph type, we first applied R function `simGraph` to simulate two  $p \times p$  matrices  $A_0$  and  $B^{(l)}$  ( $l = 1, 2, 3$ ), where  $A_0$  acts as the “baseline” structure and  $B^{(l)}$  characterizes the “deviation” from the baseline in graph  $l$ . The adjacency matrix  $A^{(l)}$  was constructed as  $A^{(l)} = 1(A_0 = B^{(l)})$ . Given  $A^{(l)}$ , we then simulated the nodes values  $\mathbf{X}$  using R function `XMRFSim`. We run 100 repetitions in each graph-type case. The specification of the tuning and algorithm

Table 2: Simulation schemes for multiple graph models

graph type	n	p	total edges	non-zero edges			different edge patterns in each pair of graphs		
				G1	G2	G3	G1:G2	G1:G3	G2:G3
GGM	100	50	1225	224	224	225	66	65	69
PGM	50	50	1225	297	280	276	59	68	59

parameters in PANDA are summarized in Table 3.

We define “Positive” as detecting a different edge pattern between two nodes in a pair of graphs and plot the sum of false positives vs. the sum of true positives over the 3 pairs of graphs in Figure 3. As expected, the naïve differencing approach performed the worst in both GGM and PGM, with lower true positives (TP) for a given false positive (FP compared to the joint training



Table 3: Tuning and algorithm parameters in PANDA for estimating multiple graphs

graph	$\gamma$	$\sigma^2$	$\lambda_2$	$T$	$n_{e,1}(\text{JGL})$	$n_{e,2}(\text{JGL})$	$n_{e,1}(\text{JFR})$	$n_{e,2}(\text{JFR})$	$m$	$\tau_0$
GGM (NS)	1	0	$\lambda_1/4$	80	4,000	4,000	2,000	2,000	1	$10^{-4}$
GGM (SCIO)	1	0	$\lambda_1/4$	150	2,000	2,000	2,000	2,000	1	$10^{-4}$
PGM (NS)	1	0	$\lambda_1/4$	80	4,000	4,000	2,000	2,000	2	$10^{-4}$

methods (PANDA, joint graphical lasso, and SGL), especially in the case of PGM. For GGMs, PANDA-JFR-NS, NS with SGL penalty, and the joint graphical lasso with the FL penalty seem to be the best at the small FP range, immediately followed by the joint graphical lasso approach with the fused lasso penalty. There were minimal differences among PANDA-NS-JGL, PANDA-SCIO-JGL and PANDA-SCIO-JFR in constructing GGMs in this simulation setting, which were slightly better than the joint graphical lasso approach with the GL penalty when FP increased.

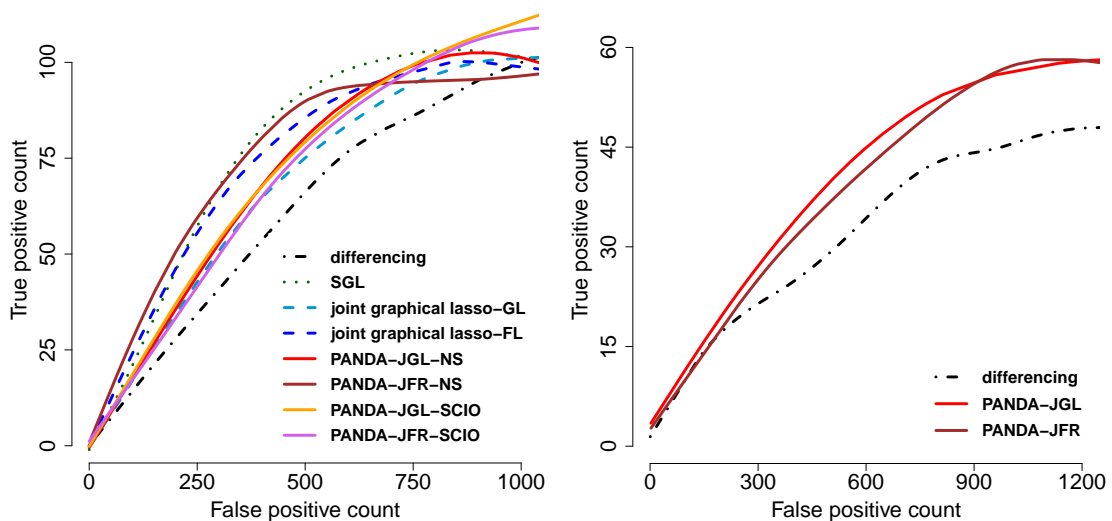


Figure 3: ROC curves in estimating three GGMs (left) and three PGMs (right)

## 4 Case study: the lung cancer microarray data

To demonstrate the use of the PANDA technique in the estimation and differentiation of multiple UGMs, we apply PANDA to a real-life data set with protein expression levels of subjects diagnosed with acute myeloid leukemia (AML). The data set is available from the [MD Anderson Department of Bioinformatics and Computational Biology](#). The subjects in the data are classified by AML subtype according to the French-American-British (FAB) classification system based on the criteria including cytogenetics and cellular morphology. We focused on 4 AML subtypes out of the 11 subtypes recorded in the data, M0 (17 subjects), M1 (34 subjects), M2 (68 subjects), and M4 (59 subjects). Data on the other 7 AML subtypes were not used because of the small sample sizes of these subtypes ( $5 \sim 13$ ).

The similarity across the protein networks from difference AML subtypes are often of interest, as the knowledge about common protein interactions across various AML subtypes can be helpful for developing treatments for AML. PANDA was used to jointly construct 4 GGMs for the 4 AML subtypes (M0, M1, M2, M4) among 18 proteins (nodes) that are known to be involved in

the apoptosis and cell cycle regulation according to the KEGG database (Kanehisa et al., 2011). The protein expression levels of the 18 proteins were assumed to follow Gaussian distributions. Because the main objective was to find common edges across the 4 GGMs, the JGL regularization was used to promote similar non-zero patterns. We set both  $n_{1,e}$  and  $n_{2,e}$  at 600. For the tuning parameters, we specified  $\gamma = 1$  and  $\sigma = 0$  to obtain a lasso-type penalty and selected  $\lambda_1^{(1)} = .005$ ,  $\lambda_1^{(2)} = 0.010$ ,  $\lambda_1^{(3)} = 0.022$ ,  $\lambda_1^{(4)} = 0.022$  and  $\lambda_2 = 0.018$  using the EBIC criterion with a grid search. We ran 50 iterations in R (version 3.4.0 (R Core Team, 2017)) on the Linux x86\_64 operating system. The computation took approximately 46 seconds.

Figure 4 displays the four GGMs estimated using PANDA. The red edges indicate protein interactions common to all 4 AML subtypes (M0, M1, M2 and M4). For example, proteins “PTEN” and “BAD.p155” were related, and so were “PTEN.p” and “BAD.p136”, which are consistent with the previous findings (Peterson et al., 2015). These common edges in the estimated graphs shed light on the similarities in the structures of the protein networks across AML different subtypes, which in turn could be to guide treatment development for AML.

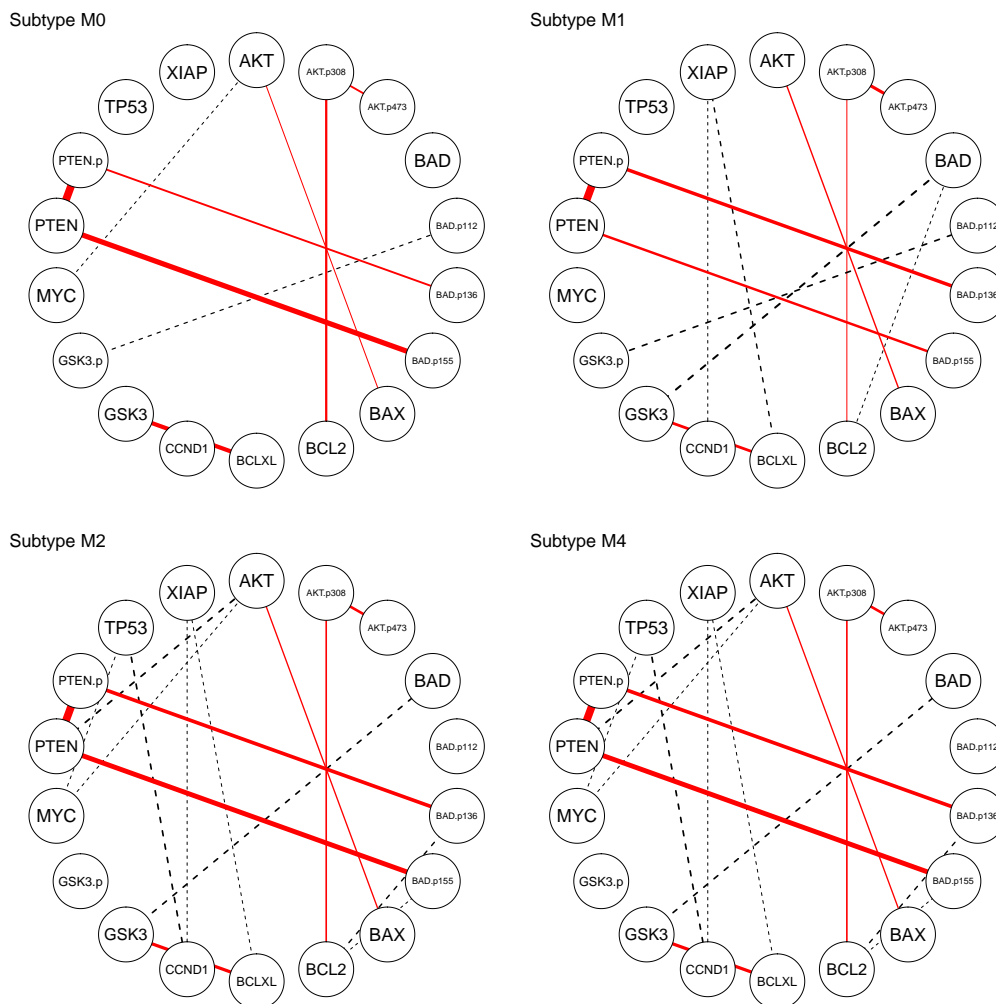


Figure 4: Four GGMs estimated jointly via PANDA-JGL in the four subtypes of AML (the edge width is proportional to its weight; the red edges are common to all 4 UGMs while the dashed black edges are not).

## 5 Discussion

We extend the data augmentation regularization technique PANDA into jointly estimating multiple graphs. Toward that end, we design two types of noises augment the observed graphs. The first type regularizes each graph, such as with sparsity; while the second type promotes either the structural similarity (the JGL regularization) or the numerical similarity (the JFR regularization) among the edges in the same positions across the graphs.

To the best our knowledge, our extension of PANDA to the multiple graph setting offers the first approach for jointly constructing multiple UGMs in general (GGMs and MGMs included), as long as each node in the graph given the other nodes can be modelled by the Exponential family and the GLMs. For general UGMs, we use the NS framework to estimate the model parameters; for GGMs, besides the NS framework, there are other alternatives such as through the Cholesky decomposition of the precision matrix or through the SCIO estimator. In all cases, we establish the expected regularization through noise augmentation. Computationally, PANDA for multiple graph estimation runs GLMs to obtain MLE iteratively on the augmented combined data across graphs, which can be programmed with a few lines in any software that offers built-in GLM functions. When the augmented data are large, the computation could take some time but usually the PANDA algorithms converge in a few iterations.

As mentioned in Sec 1, the multiple graph version of PANDA enjoys the theoretical properties established by Li et al. (2018) in the single graph setting, including the almost sure (a.s) convergence of the noise-augmented loss function to its expectation, which is a penalized loss function with the designed regularization effect, and the a.s convergence of the minimizer of the former to the minimizer of the latter. Yang et al. (2014) and Yang et al. (2015a) connect the node-wise conditional Exponential distribution with UGMs and show the graph constructed by minimizing the regularized loss function, with separate  $l_1$  penalty terms placed on the coefficients associated with the same type of nodes, is structurally consistent for the underlying UGM in the single graph setting. Danaher et al. (2014), while proposing the popular joint graphical lasso for jointly estimating multiple GGMs, do not investigate whether the estimated graphs are structurally consistent for true graph structures. Given the limitation of the previous work on structural consistency, together with the fact that jointly constructing multiple UGMs with various penalty terms on the model parameter, where the nodes do not have to be Gaussian nor of the same type, is a more difficult graph estimation problem, it implies the establishment of the structural consistency of the estimated graphs can be challenging for PANDA, or other any joint estimation approaches for the same reasons; and but can be a future research direction.

## A Proof of Corollary 1

$$\begin{aligned}
\mathbb{E}_e(l_p(\Theta|\mathbf{x}, \mathbf{e}_1, \mathbf{e}_2)) &= \sum_{l=1}^q \sum_{i=1}^{n_l} \sum_{j=1}^p \left( x_{ij}^{(l)} - \sum_{k \neq j} x_{ik}^{(l)} \theta_{jk}^{(l)} \right)^2 + \mathbb{E}_e \sum_{h=1}^2 \sum_{i=1}^{n_{e,h}} \sum_{j=1}^p \left( e_{ijj,h} - \sum_{l=1}^q \sum_{j \neq k} e_{ijk,h}^{(l)} \theta_{jk}^{(l)} \right)^2 \\
&= l(\Theta|\mathbf{x}) + \sum_{h=1}^2 \sum_{i=1}^{n_{e,h}} \sum_{j=1}^p \sum_{l=1}^q \sum_{j \neq k} \mathbb{E}_e \left( e_{ijk,h}^{(l)} \right) \theta_{jk}^{2(l)} \\
\text{JGL:} &= l(\Theta|\mathbf{x}) + \sum_{l=1}^q \lambda_1^{(l)} n_{e,1} \sum_{j=1}^p \sum_{j \neq k} \left| \theta_{jk}^{(l)} \right|^{2-\gamma} + \sum_{j=1}^p \lambda_2 n_{e,2} \omega_{jj} \sum_{j \neq k} \sum_{l=1}^q \theta_{jk}^{2(l)} \left( \sum_{l=1}^q \theta_{jk}^{2(l)} \right)^{-1/2}
\end{aligned}$$

$$\begin{aligned}
&= l(\Theta|\mathbf{x}) + \sum_{l=1}^q \lambda_1^{(l)} n_{e,1} \sum_{j=1}^p \sum_{j \neq k} \left| \theta_{jk}^{(l)} \right|^{2-\gamma} + \sum_{j=1}^p \lambda_2 n_{e,2} \omega_{jj} \sum_{j \neq k} \left( \sum_{l=1}^q \theta_{jk}^{2(l)} \right)^{1/2}; \\
\text{JFR: } &= l(\Theta|\mathbf{x}) + n_{e,1} \sum_{j=1}^p \sum_{l=1}^q \sum_{j \neq k} \mathbb{E}_{\mathbf{e}} \left( e_{ijk,1}^{2(l)} \right) \theta_{jk}^{2(l)} \\
&\quad + n_{e,2} \sum_{j=1}^p \sum_{j \neq k} \left( \sum_{l=1}^q \mathbb{E}_{\mathbf{e}} \left( e_{ijk,2}^{2(l)} \right) \theta_{jk}^{2(l)} + \sum_{l=1}^q \sum_{v=l-1} 2 \mathbb{E}_{\mathbf{e}} \left( e_{ijk,2}^{(l)} e_{ijk,2}^{(v)} \right) \theta_{jk}^{(l)} \theta_{jk}^{(v)} \right) \\
&= l(\Theta|\mathbf{x}) + \sum_{l=1}^q \lambda_1^{(l)} n_{e,1} \sum_{j=1}^p \sum_{j \neq k} \left| \theta_{jk}^{(l)} \right|^{2-\gamma} + \sum_{j=1}^p \lambda_2 n_{e,2} \omega_{jj}^2 \sum_{k \neq j} \sum_{l=1}^q \sum_{v=l-1} \left( \theta_{jk}^{(l)} - \theta_{jk}^{(v)} \right)^2
\end{aligned}$$

## B Proof of Proposition 1

The proof is straightforward by combining the proof for Corollary 1 on the regularization effects of PANDA-JGL and PANDA-JFR in multiple GGMs and the proof for Proposition 2 in Section 2.1.3 of Li et al. (2018) that establishes the regularization effect of PANDA for a single UGM in the GLM framework.

## C Proof of Proposition 3

$$\begin{aligned}
&\mathbb{E}_{\mathbf{e}}(l_p(\Theta|\mathbf{x}, \mathbf{e}_1, \mathbf{e}_2)) = \frac{1}{2n} \sum_{j=1}^p \Theta_j \mathbb{E}_{\mathbf{e}} \left( \tilde{\mathbf{x}}_j^T \tilde{\mathbf{x}}_j \right) \Theta_j - \sum_{j=1}^p \Theta_j \mathbf{B}_j \\
&= \sum_{j=1}^p \Theta_j \left( \frac{1}{2n} \mathbf{x}_j^T \mathbf{x}_j + \mathbb{E}_{\mathbf{e}} \left( \mathbf{e}_{j,1}^T \mathbf{e}_{j,1} \right) + \mathbb{E}_{\mathbf{e}} \left( \mathbf{e}_{j,2}^T \mathbf{e}_{j,2} \right) \right) \Theta_j - \sum_{j=1}^p \Theta_j \mathbf{B}_j \\
&= \frac{1}{2n} \sum_{j=1}^p \Theta_j (\mathbf{x}_j^T \mathbf{x}_j) \Theta_j - \sum_{j=1}^p \Theta_j \mathbf{B}_j + \sum_{j=1}^p \sum_{k \neq j} \sum_{h=1}^2 n_{e,h} \sum_{l=1}^q \sum_{v=\{l-1, l, l+1\}} \text{Cov} \left( e_{ijk,h}^{(l)} e_{ijk,h}^{(v)} \right) \theta_{jk}^{(l)} \theta_{jk}^{(v)} \\
&= l(\Theta|\mathbf{x}) + \lambda_1 n_{e,1} \sum_{j=1}^p \sum_{j \neq k} \sum_{l=1}^q \left| \theta_{jk}^{(l)} \right|^{2-\gamma} + \begin{cases} \lambda_2 n_{e,2} \sum_{j=1}^p \sum_{j \neq k} \left( \sum_{l=1}^q \theta_{jk}^{2(l)} \right)^{1/2} & \text{for JGL} \\ \lambda_2 n_{e,2} \sum_{j=1}^p \sum_{k \neq j} \sum_{l=1}^q \sum_{v=l-1} \left( \theta_{jk}^{(l)} - \theta_{jk}^{(v)} \right)^2 & \text{for JFR} \end{cases}
\end{aligned}$$

## D Bayesian prior for JFR/SFR regularization in Eqns (25) and (27)

We provide here the proof of Eqn (27), which can be similarly carried on to the proof of Eqn (25). Notice that prior Eqn (27) consists of independent Gaussian bridge priors for each parameter  $\theta_{jk}^{(l)}, l = 1, \dots, q$  and a joint multivariate Gaussian fused ridge prior for the parameter vector  $(\theta_{jk}^{(1)}, \dots, \theta_{jk}^{(q)})$ . To obtain fused ridge regularization terms, the direct prior would be

$$\left( \theta_{jk}^{(1)} - \theta_{jk}^{(2)}, \dots, \theta_{jk}^{(q)} - \theta_{jk}^{(1)} \right) \sim N \left( 0, \lambda_2^{-1} I_q \right), \text{ where } I_q \text{ is the identity matrix}$$

Since  $(\theta_{jk}^{(1)}, \dots, \theta_{jk}^{(q)}) \mathbf{T} = (\theta_{jk}^{(1)} - \theta_{jk}^{(2)}, \dots, \theta_{jk}^{(q)} - \theta_{jk}^{(1)})$ , where  $\mathbf{T}$  has entries  $T_{kk} = 1, T_{k+1-k \cdot 1(k=q), k} = -1$  for  $k = 1, \dots, q$ ; and 0 otherwise, we could obtain the prior on  $(\theta_{jk}^{(1)}, \dots, \theta_{jk}^{(q)})$  with the re-parameterization. Specifically,

$$\begin{aligned} & \pi(\theta_{jk}^{(1)} - \theta_{jk}^{(2)}, \dots, \theta_{jk}^{(q)} - \theta_{jk}^{(1)}) \\ & \propto \exp \left\{ -2^{-1} \lambda_2 (\theta_{jk}^{(1)} - \theta_{jk}^{(2)}, \dots, \theta_{jk}^{(q)} - \theta_{jk}^{(1)})^T I_p (\theta_{jk}^{(1)} - \theta_{jk}^{(2)}, \dots, \theta_{jk}^{(q)} - \theta_{jk}^{(1)}) \right\} \\ & = \exp \left\{ -2^{-1} \lambda_2 \boldsymbol{\theta}_{jk}^{(t)} \mathbf{T} \mathbf{T}^T \boldsymbol{\theta}_{jk}^{(t)T} \right\} \triangleq \pi(\theta_{jk}^{(1)}, \dots, \theta_{jk}^{(q)}). \end{aligned}$$

$\mathbf{T} \mathbf{T}^T$  can be regarded as the precision matrix for  $(\theta_{jk}^{(1)}, \dots, \theta_{jk}^{(q)})$  with rank  $q - 1$ . Taken together the JFR prior from the above with a sparsity prior  $(\theta_{jk}^{(1)}, \dots, \theta_{jk}^{(q)})$ , for example the prior  $\exp \left\{ -2^{-1} \left( \sum_{l=1}^q \lambda_1^{(l)} \frac{\theta_{jk}^{(l)2}}{|\theta_{jk}^{(l)(t)}|^\gamma} \right) \right\}$  that gives the bridge-type regularization, we have

$$\begin{aligned} \pi(\theta_{jk}^{(1)}, \dots, \theta_{jk}^{(q)}) & \propto \exp \left\{ -2^{-1} \left( \sum_{l=1}^q \lambda_1^{(l)} \frac{\theta_{jk}^{(l)2}}{|\theta_{jk}^{(l)(t)}|^\gamma} + \lambda_2 \boldsymbol{\theta}_{jk}^{(t)} \mathbf{T} \mathbf{T}^T \boldsymbol{\theta}_{jk}^{(t)T} \right) \right\} \\ & = \exp \left\{ -2^{-1} \left( \boldsymbol{\theta}_{jk}^{(t)} \left( \lambda_2 \mathbf{T} \mathbf{T}^T + \mathbf{diag} \left( \frac{\lambda_1^{(1)}}{|\theta_{jk}^{(1)(t)}|^\gamma}, \dots, \frac{\lambda_1^{(q)}}{|\theta_{jk}^{(q)(t)}|^\gamma} \right) \right) \boldsymbol{\theta}_{jk}^{(t)T} \right) \right\} \end{aligned}$$

## References

- Allen, G. I. and Liu, Z. (2012). A log-linear graphical model for inferring genetic networks from high-throughput sequencing data. *IEEE International Conference on Bioinformatics and Biomedicine*, pages 1–6.
- Casella, G., Ghosh, M., Gill, J., and Kyung, M. (2010). Penalized regression, standard errors, and bayesian lassos. *Bayesian Analysis*, 5(2):369–411.
- Danaher, P. (2013). *JGL: Performs the Joint Graphical Lasso for sparse inverse covariance estimation on multiple classes*. R package version 2.3.
- Danaher, P., Wang, P., and Witten, D. M. (2014). The joint graphical lasso for inverse covariance estimation across multiple classes. *J. Roy. Statist. Soc. Ser. B*, 76:373–397.
- Fellinghauer, B., Büllhlmann, P., Ryffel, M., von Rhein, M., and Reinhardt, J. D. (2013). Stable graphical model estimation with random forests for discrete, continuous, and mixed variables. *Computational Statistics and Data Analysis*, 64:132–142.
- Hoeffling, H. (2009). A path algorithm for the fused lasso signal approximator. *Journal of Computational and Graphical Statistics*, 19(4):984–1006.
- Hoffing, H. and Tibshirani, R. J. (2009). Estimation of sparse binary pairwise markov networks using pseudo-likelihoods. *The Journal of Machine Learning Research*, 10:883–906.
- Huang, J., Liu, N., Pourahmadi, M., and Liu, L. (2006). Covariance matrix selection and estimation via penalised normal likelihood. *Biometrika*, 93:85–98.
- Jalali, A., Ravikumar, P. K., Vasuki, V., and Sanghavi, S. (2011). On learning discrete graphical models using group-sparse regularization. *International Conference on Artificial Intelligence and Statistics*, pages 378–387.

- Kanehisa, M., Goto, S., Sato, Y., Furumichi, M., and Tanabe, M. (2011). Kegg for integration and interpretation of large-scale molecular data sets. *Nucleic acids research*, 40(D1):D109–D114.
- Kuang, Z., Geng, S., and Page, D. (2017). A screening rule for  $l_1$ -regularized ising model estimation. *Neural Information Processing Systems*.
- Li, Y., Liu, X., and Liu, F. (2018). Panda: Adaptive noisy data augmentation for regularization of undirected graphical models. *arXiv:1810.04851*.
- Liu, W. and Xi, L. (2015). Fast and adaptive sparse precision matrix estimation in high dimensions. *Journal of Multivariate Analysis*, 135:153 – 162.
- Peng, J., Wang, P., Zhou, N., and Zhu, J. (2009). Partial correlation estimation by joint sparse regression models. *Journal of the American Statistical Association*, 104:735–746.
- Peterson, C., Stingo, F. C., and Vannucci, M. (2015). Bayesian inference of multiple gaussian graphical models. *Journal of the American Statistical Association*, 110(509):159–174.
- R Core Team (2017). *R: A Language and Environment for Statistical Computing*. R Foundation for Statistical Computing, Vienna, Austria.
- Ravikumar, P., Wainwright, M. J., and Lafferty, J. D. (2010). High-dimensional ising model selection using  $\ell_1$ -regularized logistic regression. *Ann. Statist.*, 38(3):1287–1319.
- Simon, N., Friedman, J., Hastie, T., and Tibshirani, R. (2013). A sparse-group lasso. *Journal of Computational and Graphical Statistics*, 22(2):231–245.
- Tibshirani, R., Saunders, M., Rosset, S., Zhu, J., and Knight, K. (2005). Sparsity and smoothness via the fused lasso. *Journal of the Royal Statistical Society, Series B*, 67(1):97–108.
- Yang, E., Allen, G. I., Liu, Z., and Ravikumar, P. K. (2012). Graphical models via generalized linear models. *Advances in Neural Information Processing Systems*, 25:1367–1375.
- Yang, E., Allen, G. I., Liu, Z., and Ravikumar, P. K. (2014). Mixed graphical models via exponential families. *Proceedings of the Seventeenth International Conference on Artificial Intelligence and Statistics*, pages 1042–1050.
- Yang, E., Ravikumar, P., Allen, G. I., and Liu, Z. (2015a). Graphical models via univariate exponential family distributions. *Journal of Machine Learning Research*, 16:3813–3847.
- Yang, S., Lu, Z., Shen, X., Wonka, P., and Ye, J. (2015b). Fused multiple graphical lasso. *Siam Journal on Optimization*, 25(2):916–943.
- Yuan, M. (2010). High dimensional inverse covariance matrix estimation via linear programming. *Journal of Machine Learning Research*, 11:2261–2286.
- Zhang, Y., Ouyang, Z., and Zhao, H. (2017). A statistical framework for data integration through graphical models with application to cancer genomics. *The Annals of Applied Statistics*, 11(1):161–184.



## Supplementary Materials to

*AdaPtive Noisy Data Augmentation (PANDA) for Simultaneous*

*Construction Multiple Graph Models*

Yinan Li<sup>1</sup>, Xiao Liu<sup>2</sup>, and Fang Liu<sup>1</sup>

<sup>1</sup> Department of Applied and Computational Mathematics and Statistics

<sup>2</sup> Department of Psychology

University of Notre Dame, Notre Dame, IN 46556, U.S.A.

## S.1 PANDA-CD Algorithm for multiple GGM estimation

---

**Algorithm 1** PANDA-CD for joint estimation of  $q$  GGMs

---

- 1: **Input:**
    - random initial estimates  $\bar{\boldsymbol{\theta}}_j^{(l)(0)}$  for  $j = 1, \dots, p$  and  $l = 1, \dots, q$ .
    - a NGD for generating  $e_1$  with proper tuning parameters (Table 1), a NGD for  $e_2$  with proper tuning parameters (Eqn (3) for PANDA-JGL and Eqn (4) for PANDA-JFR), maximum iteration  $T$ , noisy data sizes  $n_{e,1}$  and  $n_{e,2}$ , thresholds  $\tau, \tau_0$ , width of moving average (MA) window  $m$ , banked parameter estimates after convergence  $r$ , inner loop  $K$  in alternatively estimating  $\boldsymbol{\theta}_j$  and  $\sigma_j^2$
  - 2:  $t \leftarrow 0$ ; convergence  $\leftarrow 0$
  - 3: **WHILE**  $t < T$  **AND** convergence = 0
  - 4:   **FOR**  $j = 2$  to  $p$
  - 5:    **FOR**  $k = 1 : K$ 
    - a) Generate  $e_{ijk,1}^{(l)}$  for  $i = 1, \dots, n_{e,1}$ , and  $e_{ijk,2}^{(l)}$  for  $i = 1, \dots, n_{e,2}$ , with  $\bar{\boldsymbol{\theta}}_j^{(l)(t-1)}$  plugged in the variance terms of the NGDs. to obtain augmented data as depicted in Figure 2.
    - c) Obtain the OLS estimates  $\hat{\boldsymbol{\theta}}_j^{(t)} = (\hat{\boldsymbol{\theta}}_j^{(1)(t)}, \dots, \hat{\boldsymbol{\theta}}_j^{(q)(t)})$  by regressing  $\tilde{\mathbf{x}}_j = \tilde{\mathbf{x}}_{1:j-1}^{(1)} \boldsymbol{\theta}_j^{(1)} + \dots, + \tilde{\mathbf{x}}_{1:j-1}^{(q)} \boldsymbol{\theta}_j^{(q)}$ .
    - d) If  $t > m$ , calculate the MA  $\bar{\boldsymbol{\theta}}_j^{(l)(t)} = m^{-1} \sum_{b=t-m+1}^t \hat{\boldsymbol{\theta}}_j^{(l)(b)}$ ; otherwise  $\bar{\boldsymbol{\theta}}_j^{(l)(t)} = \hat{\boldsymbol{\theta}}_j^{(l)(t)}$  for  $l = 1, \dots, q$ . Calculate the sum of squared error  $\text{SSE}_j^{(t)}$  given  $\bar{\boldsymbol{\theta}}_j^{(t)}$  and  $\hat{\sigma}_j^{2(t)} = \text{SSE}_j^{(t)}/3n$ .
  - 6:    **End FOR**
  - 7:    Calculate the overall loss function  $\bar{l}^{(t)} = \sum_{j=1}^p \text{SSE}_j^{(t)}$  and apply one of the convergence
  - 8:    criteria to  $\bar{l}^{(t)}$ . Let convergence  $\leftarrow 1$  if the convergence is reached.
  - 9:    **End WHILE**
  - 10: Continue to execute the command lines 4 and 6 for another  $r$  iterations, and record  $\bar{\boldsymbol{\theta}}_j^{(l)(b)}$  for  $b = t+1, \dots, t+r$  and  $l = 1, \dots, q$ , calculate the degrees of freedom  $\nu_j^{(t)} = \text{trace}(\mathbf{x}_j (\tilde{\mathbf{x}}_j' \tilde{\mathbf{x}}_j)^{-1} \mathbf{x}_j')$  and  $\hat{\sigma}_j^{2(b)} = \text{SSE}_j^{(t)}/(n - \nu_j^{(b)})$ . Let  $\bar{\boldsymbol{\theta}}_{jk}^{(l)} = (\bar{\boldsymbol{\theta}}_{jk}^{(l)(t+1)}, \dots, \bar{\boldsymbol{\theta}}_{jk}^{(l)(t+r)})$ .
  - 11: Set  $\hat{\boldsymbol{\theta}}_{jk}^{(l)} = 0$  if  $(|\max\{\bar{\boldsymbol{\theta}}_{jk}^{(l)}\} \cdot \min\{\bar{\boldsymbol{\theta}}_{jk}^{(l)}\}| < \tau_0) \cap (\max\{\bar{\boldsymbol{\theta}}_{jk}^{(l)}\} \cdot \min\{\bar{\boldsymbol{\theta}}_{jk}^{(l)}\}) < 0$  for  $k > j$ ; otherwise, set  $\hat{\boldsymbol{\theta}}_{jk} = r^{-1} \sum_{b=t+1}^{t+r} \bar{\boldsymbol{\theta}}_{jk}^{(b)(l)}$ . Set  $\hat{D} = r^{-1} \sum_{b=t+1}^{t+r} \mathbf{diag}(\hat{\sigma}_1^{2(b)}, \dots, \hat{\sigma}_p^{2(b)})$ . Calculate  $\hat{\Omega}^{(l)} = \hat{L}^{(l)'} \hat{D} \hat{L}^{(l)}$
  - 12: **Output:**  $\hat{\Omega}^{(l)}$ .
-

## S.2 PANDA-SCIO Algorithm for multiple GGM estimation

---

**Algorithm 2** PANDA-SCIO for joint estimation of  $q$  GGMs

---

- 1: **Pre-processing:** standardize  $\mathbf{x}^{(l)}$  for  $l = 1, 2, 3$  separately.
  - 2: **Input:**
    - random initial estimates  $\bar{\boldsymbol{\theta}}_j^{(l)(0)}$  for  $j = 1, \dots, p$  and  $l = 1, \dots, q$ .
    - a NGD for generating  $e_1$  with proper tuning parameters (Table 1), a NGD for  $e_2$  with proper tuning parameters (Eqn (20) for PANDA-JGL and Eqn (21) for PANDA-JFR), maximum iteration  $T$ , noisy data sizes  $n_{e,1}$  and  $n_{e,2}$ , thresholds  $\tau, \tau_0$ , width of moving average (MA) window  $m$ , banked parameter estimates after convergence  $r$ .
  - 3:  $t \leftarrow 0$ ; convergence  $\leftarrow 0$
  - 4: **WHILE**  $t < T$  **AND** convergence = 0
  - 5:   **FOR**  $j = 1 : p$ 
    - a) Generate  $e_{ijk,1}^{(l)}$  for  $i = 1, \dots, n_{e,1}$ , and  $e_{ijk,2}^{(l)}$  for  $i = 1, \dots, n_{e,2}$ , with  $\bar{\boldsymbol{\theta}}_j^{(l)(t-1)}$  plugged in the variance terms of the NGDs.
    - b) Obtain augmented data  $\tilde{\mathbf{x}}$  by combining the standardized  $\mathbf{x}^{(l)}$  and the  $\sqrt{2n_{e,1}}\mathbf{e}_{j,1}, \sqrt{2n_{e,2}}\mathbf{e}_{j,2}$  from a) according to Figure 1.
    - c) Calculate  $\hat{\boldsymbol{\Theta}}_j^{(t)} = 2n \left( \tilde{\mathbf{x}}_j^T \tilde{\mathbf{x}}_j \right)^{-1} \mathbf{B}_j$  and obtain  $\hat{\boldsymbol{\theta}}_j^{(t)} = \left[ \hat{\boldsymbol{\theta}}_j^{(1)(t)} // \dots // \hat{\boldsymbol{\theta}}_j^{(q)(t)} \right]$ .
    - d) If  $t > m$ , calculate the MA  $\bar{\boldsymbol{\Theta}}_j^{(1)(t)} = m^{-1} \sum_{b=t-m+1}^t \hat{\boldsymbol{\Theta}}_j^{(1)(b)}$ ; otherwise  $\bar{\boldsymbol{\Theta}}_j^{(1)(t)} = \hat{\boldsymbol{\Theta}}_j^{(1)(t)}$
  - End FOR**
  - 6:   Plug in  $\bar{\boldsymbol{\Theta}}_j^{(l)(t)}$  for  $j = 1, \dots, p$  in the loss function in Eqn (22) to obtain  $\bar{l}^{(t)}$ . and apply
  - 7:   one of the convergence criteria to  $\bar{l}^{(t)}$ .
  - 8:   Let convergence  $\leftarrow 1$  if the convergence is reached.
  - 9: **End WHILE**
  - 10: Continue to execute the command line 5 for another  $r$  iterations, and record  $\bar{\boldsymbol{\Theta}}_j^{(l)(b)}$  for  $b = t+1, \dots, t+r$  and  $l = 1, \dots, q$ . Let  $\bar{\boldsymbol{\theta}}_{jk}^{(l)} = (\bar{\theta}_{jk}^{(l)(t+1)}, \dots, \bar{\theta}_{jk}^{(l)(t+r)})$ .
  - 11: Set  $\hat{\theta}_{jk}^{(l)} = \hat{\theta}_{kj}^{(l)} = 0$  if  $\left( \left| \max\{\bar{\boldsymbol{\theta}}_{jk}^{(l)}\} \cdot \min\{\bar{\boldsymbol{\theta}}_{jk}^{(l)}\} \right| < \tau_0 \right) \cap \left( \max\{\bar{\boldsymbol{\theta}}_{jk}^{(l)}\} \cdot \min\{\bar{\boldsymbol{\theta}}_{jk}^{(l)}\} < 0 \right)$  or  $\left( \left| \max\{\bar{\boldsymbol{\theta}}_{kj}^{(l)}\} \cdot \min\{\bar{\boldsymbol{\theta}}_{kj}^{(l)}\} \right| < \tau_0 \right) \cap \left( \max\{\bar{\boldsymbol{\theta}}_{kj}^{(l)}\} \cdot \min\{\bar{\boldsymbol{\theta}}_{kj}^{(l)}\} < 0 \right)$  for  $k \neq j$ ; otherwise, set  $\hat{\theta}_{jk} = \min\{\bar{\boldsymbol{\theta}}_{jk}^{(l)}, \bar{\boldsymbol{\theta}}_{kj}^{(l)}\}$ .
  - 12: Set  $\hat{\boldsymbol{\Omega}}_j^{(l)} = \hat{\boldsymbol{\theta}}_j^{(l)}$
  - 13: **Output:**  $\hat{\boldsymbol{\Omega}}^{(l)}$
-